

DOUBLE-LOOP QUASI-MONTE CARLO ESTIMATOR FOR NESTED INTEGRATION

ARVED BARTUSKA¹, ANDRÉ GUSTAVO CARLON², LUIS ESPATH³, SEBASTIAN KRUMSCHEID⁵, & RAÚL TEMPONE^{1,2,4}

ABSTRACT. Nested integration arises when a nonlinear function is applied to an integrand, and the result is integrated again, which is common in engineering problems, such as optimal experimental design, where typically neither integral has a closed-form expression. Using the Monte Carlo method to approximate both integrals leads to a double-loop Monte Carlo estimator, which is often prohibitively expensive, as the estimation of the outer integral has bias relative to the variance of the inner integrand. For the case where the inner integrand is only approximately given, additional bias is added to the estimation of the outer integral. Variance reduction methods, such as importance sampling, have been used successfully to make computations more affordable. Furthermore, random samples can be replaced with deterministic low-discrepancy sequences, leading to quasi-Monte Carlo techniques. Randomizing the low-discrepancy sequences simplifies the error analysis of the proposed double-loop quasi-Monte Carlo estimator. To our knowledge, no comprehensive error analysis exists yet for truly nested randomized quasi-Monte Carlo estimation (i.e., for estimators with low-discrepancy sequences for both estimations). We derive asymptotic error bounds and a method to obtain the optimal number of samples for both integral approximations. Then, we demonstrate the computational savings of this approach compared to standard nested (i.e., double-loop) Monte Carlo integration when estimating the expected information gain via two examples from Bayesian optimal experimental design, the latter of which involves an experiment from solid mechanics.

AMS subject classifications: · 62F15 · 65C05 · 65D30 · 65D32 ·

CONTENTS

1. Introduction	2
Greek alphabet	3
2. Brief overview of Monte Carlo and quasi-Monte Carlo integration	3
2.1. Monte Carlo method	3
2.2. Quasi-Monte Carlo method	4
3. Nested integration	5
4. Numerical results	10
4.1. Example 1: Linear example with exact sampling	12
4.2. Example 2: Thermoelasticity example with inexact sampling	14
5. Conclusion	21
6. Acknowledgments	21
Appendix A. Proof of Remark 4	21
Appendix B. Derivation of the finite element formulation	21
References	21

¹DEPARTMENT OF MATHEMATICS, RWTH AACHEN UNIVERSITY, GEBÄUDE-1953 1.OG, PONTDRIESCH 14-16, 161, 52062 AACHEN, GERMANY

²KING ABDULLAH UNIVERSITY OF SCIENCE & TECHNOLOGY (KAUST), COMPUTER, ELECTRICAL AND MATHEMATICAL SCIENCES & ENGINEERING DIVISION (CEMSE), THUWAL 23955-6900, SAUDI ARABIA

³SCHOOL OF MATHEMATICAL SCIENCES, UNIVERSITY OF NOTTINGHAM, NOTTINGHAM, NG7 2RD, UNITED KINGDOM

⁴ALEXANDER VON HUMBOLDT PROFESSOR IN MATHEMATICS FOR UNCERTAINTY QUANTIFICATION, RWTH AACHEN UNIVERSITY, GERMANY

⁵STEINBUCH CENTER FOR COMPUTING, AND INSTITUTE FOR APPLIED AND NUMERICAL MATHEMATICS, KARLSRUHE INSTITUTE OF TECHNOLOGY, GERMANY

E-mail address: bartuska@uq.rwth-aachen.de.

Date: March 1, 2023.

1. INTRODUCTION

A nested integral is an integral of a usually nonlinear function of another parametric integral. Integrals of this type appear in many fields (e.g., geology [21], mathematical finance [22], medical decision-making [23], and optimal experimental design (OED) [1]). The Monte Carlo (MC) method is one of the most popular approximation techniques for integrals, especially high-dimensional ones. For nested integrals, both can be approximated using the MC method, resulting in the double-loop MC (DLMC) estimator. Using MC to approximate a single integral to a specified error tolerance $TOL > 0$ requires a sample size of $\mathcal{O}(TOL^{-2})$, whereas using DLMC results in worse complexity, with an overall number of samples of $\mathcal{O}(TOL^{-3})$ [1]. The two MC estimators in the DLMC estimator are connected through a nonlinear function; thus, the statistical error of the inner MC estimator causes bias in the DLMC estimator. The sample sizes of both MC estimators must be carefully controlled to guarantee that the error in the DLMC estimator is below TOL with a certain confidence, controlling both the statistical error and bias. Improving the DLMC performance is the goal of intense research, with some approaches proposing the use of Laplace approximation [7], importance sampling [2], and multilevel MC (MLMC) [23].

The randomized quasi-MC (RQMC) method [24, 25, 26, 27, 31, 39] is a promising technique to improve the efficiency of the basic MC method (i.e., the required number of samples to meet a certain tolerance) while maintaining nonintrusive sampling. The RQMC estimator uses deterministic points from a low-discrepancy sequence and randomizes the entire sequence while maintaining a low-discrepancy structure. Randomization allows for the use of either the central limit theorem or Chebyshev inequality to estimate and subsequently bound the error asymptotically [28, 36, 39]. Given appropriate regularity assumptions on the integrand, the RQMC method can reduce the order of convergence of the approximation error without introducing additional bias to the MC estimator. Furthermore, if the integrand is sufficiently smooth, this approach can yield an asymptotic rate of 1 as the number of low-discrepancy points increases. The number of evaluations needed by the RQMC estimator to achieve a tolerance TOL is $\mathcal{O}(TOL^{-1})$.

Recently, researchers [37] have investigated the optimal error tolerance that can be achieved by RQMC, given a fixed number of samples and a certain confidence level. They demonstrated that combining RQMC with robust estimation improves error tolerances. The RQMC concepts have been applied in the context of OED in [35], but only to the outer integral of a nested integration problem. In [35], the inner integral is approximated using the MC method. A reduced sample standard deviation was observed for several numerical experiments for this scheme compared to using the MC method for both integrals, which was demonstrated for a fixed number of outer and inner samples.

In recent work [23], an RQMC method was used to approximate the outer integral of a nested estimator in medical decision-making. The authors estimated the variance error using the sample variance and bias error by successively doubling the number of inner samples. They compared this RQMC method with an MCLC approach and standard nested (i.e., double loop) MC by specifying a target mean squared error and observing the number of samples needed until this target is reached. Both MLMC and RQMC have similar performance results in practice, depending on the number of parameters and other measures of model complexity.

In [21], nested integrals are approximated using MLMC techniques. The number of inner samples is increased for each level to reduce the bias induced on the outer approximation by the variance of the inner approximation. The RQMC estimator approximates the inner integral and reduces the variance, requiring a smaller sample size in the inner loop to achieve the error tolerance in the MLMC setting specified in [19, Theorem 3.1]. This outcome is presented both theoretically and via examples. A similar approach is followed in [22]. In this study, a discontinuous inner integrand is approximated using a sigmoid (i.e., smooth function), allowing the RQMC method to be applied.

To further reduce the number of samples required to estimate nested integrals up to a specified error tolerance TOL , we use RQMC for both integrals to build a double-loop quasi-MC (DLQMC) estimator. Indeed, under suitable regularity conditions, the DLQMC method can significantly reduce the required number of overall samples to $\mathcal{O}(TOL^{-1.5})$, compared to $\mathcal{O}(TOL^{-3})$ for the DLMC method. Moreover, we demonstrate that using RQMC for the outer integral has a greater effect on the overall number of samples than using it for the inner integral, but further savings can still be achieved by applying RQMC to both integrals. We also consider the case where the inner integrand is given only approximately in terms of a

computational model, resulting in additional bias for the outer approximation. We provide approximate error bounds using suitable RQMC estimators and verify them on numerical examples.

This paper provides a quick overview of the MC and quasi-MC (QMC) methods, including bounds on the absolute error in Section 2. We introduce the proposed nested RQMC estimator in Section 3. As the main contributions of this work, we derive asymptotic error bounds on the number of inner and outer samples in Propositions 1 and 2, and the optimal setting for this estimator in Proposition 3. Finally, in Section 4, we present two examples from Bayesian OED, where nested integrals frequently arise. The first example is an algebraic model introduced in [29], which can be evaluated at a low cost and serves as a toy problem to highlight the effectiveness of the proposed method. The second example demonstrates an application from solid mechanics involving the solution to a partial differential equation (PDE) with favorable regularity properties, demonstrating the practical applicability of the DLQMC estimator.

GREEK ALPHABET

α	confidence level
β	increase in convergence rate of QMC beyond MC for the outer integral
γ	work rate for the finite element method
δ	increase in convergence rate of QMC beyond MC for the inner integral
ϵ	observation noise
ε	central limit theorem error
ε	strain tensor
η	convergence rate of the discretization error
θ	parameter of interest
ϑ	dummy variable for the parameter of interest
ϑ	absolute temperature
κ	splitting parameter between bias and variance error
λ	first Lamé constant
μ	second Lamé constant
ξ	design parameter
π	probability density function of the parameter of interest
ρ	randomization
ρ	material density
σ	diagonal elements of the error covariance matrix
Σ	error covariance matrix and approximate negative inverse Hessian of the log-likelihood
Φ	cumulative distribution function of the standard normal distribution
ω	random outcome in the finite element formulation
Ω	space of outcomes in the finite element formulation

2. BRIEF OVERVIEW OF MONTE CARLO AND QUASI-MONTE CARLO INTEGRATION

Before we address the case of nested integration, which is the focus of this work, we first recall the basic concepts for approximating integrals using MC and RQMC for the reader's convenience.

2.1. Monte Carlo method. We can approximate the integral

$$(1) \quad I = \int_{[0,1]^d} g(\mathbf{x}) \, d\mathbf{x},$$

where $g : [0, 1]^d \rightarrow \mathbb{R}$ is square-integrable, and d a positive integer, using the MC estimator:

$$(2) \quad I \approx I_{\text{MC}} := \frac{1}{N} \sum_{n=1}^N g(\mathbf{x}^{(n)}).$$

The MC method uses random points $\mathbf{x}^{(1)}, \dots, \mathbf{x}^{(N)}$ that are independent and identically distributed (iid) samples from the uniform distribution $\mathcal{U}([0, 1]^d)$ to approximate I in (1). Using the central limit theorem (CLT) [30] to analyze the error of the MC estimator, we find that

$$(3) \quad \mathbb{P}(|I - I_{\text{MC}}| \leq \varepsilon_{\text{MC}}) \geq 1 - \alpha$$

where

$$(4) \quad \varepsilon_{\text{MC}} := \frac{C_\alpha \sqrt{\mathbb{V}[g]}}{\sqrt{N}},$$

as $N \rightarrow \infty$, where $C_\alpha = \Phi^{-1}(1 - \alpha/2)$, Φ^{-1} is the inverse cumulative distribution function (cdf) of the standard normal distribution, and $\mathbb{V}[g]$ is the variance of the integrand for $0 < \alpha \ll 1$. Alternatively, Chebyshev's inequality could be used to obtain an error estimate similar to (3) and (4), although with a potentially larger constant C_α .

2.2. Quasi-Monte Carlo method. The MC method always converges to the true value of the integral, even under weak assumptions, but the rate of $N^{-0.5}$ can be improved for certain integrands. We can instead use the RQMC method, which achieves a better convergence rate by exploiting the regularity properties of the integrand. For a square-integrable function $g : [0, 1]^d \rightarrow \mathbb{R}$, the RQMC estimator to approximate the integral (1) is given by

$$(5) \quad I_{\text{Q}} := \frac{1}{N} \sum_{n=1}^N g(\mathbf{x}^{(n)}),$$

where $\mathbf{x}^{(1)}, \dots, \mathbf{x}^{(N)}$ are chosen from a sequence of points consisting of a deterministic component $\boldsymbol{\xi} \in [0, 1]^d$ and a random component $\boldsymbol{\rho}$,

$$(6) \quad \mathbf{x}^{(n)} = \{\boldsymbol{\xi}^{(n)}, \boldsymbol{\rho}\}, \quad 1 \leq n \leq N.$$

In particular, choosing $\boldsymbol{\xi}^{(1)}, \dots, \boldsymbol{\xi}^{(N)}$ from a low-discrepancy sequence [26, 25] results in improved convergence for smooth integrands. One example that can achieve this is lattice rules [25], and $\boldsymbol{\rho} \sim \mathcal{U}[0, 1]^d$ is a random shift. This example provides points of the shape

$$(7) \quad \{\boldsymbol{\xi}^{(n)}, \boldsymbol{\rho}\} = \text{fr}(\boldsymbol{\xi}^{(n)} + \boldsymbol{\rho}),$$

where $\text{fr}(\cdot)$ denotes the componentwise fractional part operator. Every one-dimensional projection of this point set is injective. Another common method for selecting a suitable low-discrepancy sequence is to choose the deterministic points $\boldsymbol{\xi}^{(1)}, \dots, \boldsymbol{\xi}^{(N)}$ from a digital sequence [26, 27] and set $\boldsymbol{\rho}$ to be random permutations of the digits of $\boldsymbol{\xi}^{(1)}, \dots, \boldsymbol{\xi}^{(N)}$. By splitting $[0, 1]^d$ into equally spaced subintervals in each dimension, each subinterval contains the same number of points. We use a digital sequence called Sobol sequence [34] throughout this work, as it has performed best on numerical tests. A number of points N , such that $\log_2(N) \in \mathbb{N}$, must be used to achieve the best results for this sequence type. The difference between the estimators (2) and (5) lies in the points used to evaluate the function to be integrated.

Traditional error estimates for numerical integration based on deterministic low-discrepancy sequences (i.e., $\mathbf{x}^{(n)} = \{\boldsymbol{\xi}^{(n)}\}$ in (6)) use the Koksma–Hlawka inequality [40, 26] to bound the error by a product of suitable measures for the low-discrepancy sequence and integrand, respectively. This approach can be problematic in practice because, in most instances, sharp estimates of these quantities are exceedingly difficult to obtain, and the resulting quadrature error bound is far from optimal [39].

To obtain a probabilistic estimate using the CLT, we must use several iid randomizations $\boldsymbol{\rho}^{(r)}$, $1 \leq r \leq R$ in (6). Then, we find that

$$(8) \quad \mathbb{P}(|I - I_{\text{Q}}| \leq \varepsilon_{\text{Q}}) \geq 1 - \alpha$$

approximately holds for

$$(9) \quad \varepsilon_{\text{Q}} := \frac{C_\alpha \sqrt{\mathbb{V}[I_{\text{Q}}]}}{\sqrt{R}},$$

for $0 < \alpha \ll 1$, where the variance of the RQMC estimator can be approximated as follows:

$$(10) \quad \mathbb{V}[I_{\text{Q}}] \approx \frac{1}{R-1} \sum_{r=1}^R \left(\frac{1}{N} \sum_{n=1}^N g(\{\boldsymbol{\xi}^{(n)}, \boldsymbol{\rho}^{(r)}\}) - \bar{I}_{\text{Q}} \right)^2,$$

and

$$(11) \quad \bar{I}_{\text{Q}} := \frac{1}{R} \sum_{r=1}^R \frac{1}{N} \sum_{n=1}^N g(\{\boldsymbol{\xi}^{(n)}, \boldsymbol{\rho}^{(r)}\}).$$

For a fixed R , the error (9) decreases at the rate $\mathcal{O}\left(N^{-\frac{(1+\delta)}{2}}\right)$ for $N \rightarrow \infty$ [37, 32, 33, 39], where $0 \leq \delta \leq 1$ depends on the dimension d and may depend on the regularity of the integrand g . For $\delta = 0$, this provides the usual MC rate of $1/2$. For certain functions g with desirable properties such as smoothness and boundedness, more precise statements are possible [37, 41]. The CLT-based error estimate (8) only holds asymptotically as $R \rightarrow \infty$. It can still be used in practice to obtain a confidence interval of the error (9); however, keeping R fixed and letting $N \rightarrow \infty$ is sometimes problematic, as [28, 36] noted. Specifically, the convergence of the distribution of the estimator (5) to a normal distribution cannot be guaranteed. Chebyshev's inequality can also justify the convergence rate of $(1+\delta)/2$. We employ the CLT for the error analysis and demonstrate that the derived error bounds hold at the specified confidence level for a simple example. However, we remark that it is straightforward to adapt the analysis to the Chebyshev bounds instead.

Remark 1 (Integration over general domains). *The (RQ)-MC method is commonly defined for integration over the unit cube and uniform random variables. For integrals over general domains (e.g., normal random variables), the corresponding inverse cdf can be applied to maintain the general shape of the estimators (2) and (5).*

3. NESTED INTEGRATION

After discussing the basics of the RQMC estimator, we address the focus of this work. This section establishes the DLQMC estimator for nested integration problems, derives asymptotic error bounds in the number of samples, and analyzes the optimal work required for this estimator to meet a tolerance goal.

Definition 1 (Nested integral). *We define a nested integral as*

$$(12) \quad I = \int_{[0,1]^{d_1}} f \left(\int_{[0,1]^{d_2}} g(\mathbf{y}, \mathbf{x}) \, d\mathbf{x} \right) \, d\mathbf{y},$$

where the square-integrable function $f : \mathbb{R} \rightarrow \mathbb{R}$ is nonlinear and twice differentiable with respect to \mathbf{y} . In addition, $g : [0, 1]^{d_1} \times [0, 1]^{d_2} \rightarrow \mathbb{R}$ is square-integrable and defines a nonlinear relation between \mathbf{x} and \mathbf{y} , where d_1, d_2 are positive integers.

Example 1 (Nested integral). *The integral*

$$(13) \quad I = \int_{[0,1]^{d_1}} \log \left(\int_{[0,1]^{d_2}} \exp(\mathbf{y} \cdot \mathbf{G}(\mathbf{x})) \, d\mathbf{x} \right) \, d\mathbf{y},$$

where $\mathbf{G}(\mathbf{x})$ is a nonlinear function, is of the nested type and is typically not solvable in closed form, motivating the use of numerical integration techniques to approximate I .

A standard method to approximate a nested integral (12) is via the DLQMC estimator [1], defined as

$$(14) \quad I_{\text{DLQMC}} := \frac{1}{N} \sum_{n=1}^N f \left(\frac{1}{M} \sum_{m=1}^M g(\mathbf{y}^{(n)}, \mathbf{x}^{(n,m)}) \right),$$

where the points $\mathbf{y}^{(n)}$, $1 \leq n \leq N$, are sampled iid from $\mathcal{U}([0, 1]^{d_1})$, and $\mathbf{x}^{(n,m)}$, $1 \leq n \leq N$, $1 \leq m \leq M$, are sampled iid from $\mathcal{U}([0, 1]^{d_2})$. The standard MC estimator (2) for a single integral is unbiased and has a variance that decreases with the number of samples, which holds for the inner MC estimator in (14), where the variance decreases with the number of inner samples M . The outer MC estimator in (14) has a variance that decreases with N but also has a bias relative to the size of the variance of the inner integral estimate. Thus, we typically require many inner and outer samples to keep the bias and variance of this estimator in check, significantly limiting its practical usefulness, particularly for computationally demanding problems.

Directly evaluating the function g is often not possible. For example, if evaluating g requires solving a PDE, we may only have access to a finite element method (FEM) approximation g_h with discretization parameter h . As $h \rightarrow 0$ asymptotically, the convergence order of g_h is given by

$$(15) \quad \mathbb{E}[|g(\mathbf{y}, \mathbf{x}) - g_h(\mathbf{y}, \mathbf{x})|] = C_{\text{disc}} h^\eta + h.o.t.,$$

where $\eta > 0$ is the h -convergence rate and $C_{\text{disc}} > 0$ is a constant. The work of evaluating g_h is assumed to be $\mathcal{O}(h^{-\gamma})$, for some $\gamma > 0$.

Unless stated otherwise, we assume that a discretized g_h is used in the numerical estimators and omit the subscript for concision. The DLMC estimator has a bias with the following upper bound:

$$(16) \quad |\mathbb{E}[I_{\text{DLMC}}] - I| \leq C_{\text{disc}} h^\eta + \frac{C_{\text{MC},3}}{M} + o(h^\eta) + \mathcal{O}\left(\frac{1}{M^2}\right),$$

where $C_{\text{MC},3} > 0$ is a constant related to the variance of the inner MC estimation in (14), and $C_{\text{disc}} > 0$ might be different from the one introduced in (15). The DLMC estimator has a variance with the following upper bound:

$$(17) \quad \mathbb{V}[I_{\text{DLMC}}] \leq \frac{C_{\text{MC},1}}{N} + \frac{C_{\text{MC},2}}{NM} + \mathcal{O}\left(\frac{1}{NM^2}\right),$$

where $C_{\text{MC},1}, C_{\text{MC},2} > 0$ are constants [2]. The optimal work of the DLMC estimator for a specified error tolerance $TOL > 0$ is given by

$$(18) \quad W_{\text{DLMC}}^* \propto TOL^{-(3+\frac{2}{\eta})}.$$

Proofs for the specific case of approximating the expected information gain (EIG) in Bayesian OED are presented in [2], but adapting them to the general case is straightforward.

To obtain smaller error bounds and, subsequently, smaller optimal work, we replaced both MC approximations in (14) with RQMC approximations and arrived at the DLQMC estimator, which we define below.

Definition 2 (DLQMC estimator). *The DLQMC estimator of a nested integral (12) is defined as follows:*

$$(19) \quad I_{\text{DLQ}} := \frac{1}{N} \sum_{n=1}^N f\left(\frac{1}{M} \sum_{m=1}^M g(\mathbf{y}^{(n)}, \mathbf{x}^{(n,m)})\right),$$

where the square-integrable function $f: \mathbb{R} \rightarrow \mathbb{R}$ is nonlinear, and $g: [0, 1]^{d_1} \times [0, 1]^{d_2} \rightarrow \mathbb{R}$ is square-integrable. The sample points have the following shape (see (6)):

$$(20) \quad \begin{aligned} \mathbf{y}^{(n)} &= \{\boldsymbol{\xi}_{d_1}^{(n)}, \boldsymbol{\rho}_{d_1}\}, & 1 \leq n \leq N \\ \mathbf{x}^{(n,m)} &= \{\boldsymbol{\xi}_{d_2}^{(m)}, \boldsymbol{\rho}_{d_2}^{(n)}\}, & 1 \leq n \leq N, 1 \leq m \leq M, \end{aligned}$$

where $\boldsymbol{\xi}_{d_1} \in [0, 1]^{d_1}$ and $\boldsymbol{\xi}_{d_2} \in [0, 1]^{d_2}$.

One instance of the estimator (19) requires $N+1$ iid randomizations. The total number of function evaluations required to obtain a probabilistic error estimate using iid randomizations $\boldsymbol{\rho}^{(r)} \equiv \{\boldsymbol{\rho}_{d_1}, \boldsymbol{\rho}_{d_2}^{(1)}, \dots, \boldsymbol{\rho}_{d_2}^{(n)}\}^{(r)}$, $1 \leq r \leq R$, is $N \times M \times R$. The difference between the estimators (14) and (19) lies in the points used to evaluate the function to be integrated.

Next, we analyze the error of DLQMC. First, we split the error into the bias and statistical errors, respectively, and estimate each individually. Specifically, these terms are

$$(21) \quad |I_{\text{DLQ}} - I| \leq \underbrace{|\mathbb{E}[I_{\text{DLQ}}] - I|}_{\text{bias error}} + \underbrace{|I_{\text{DLQ}} - \mathbb{E}[I_{\text{DLQ}}]|}_{\text{statistical error}}.$$

The CLT allows us to replace the statistical error with the variance $\mathbb{V}[I_{\text{DLQ}}]$.

Proposition 1 (Bias of the DLQMC estimator). *The DLQMC estimator for (12) has a bias with the following upper bound:*

$$(22) \quad |\mathbb{E}[I_{\text{DLQ}}] - I| \leq C_{\text{disc}} h^\eta + \frac{C_{\text{Q},3}}{M^{(1+\delta)}} + \mathcal{O}(h^{\eta+1}) + \mathcal{O}\left(\frac{1}{M^{2(1+\delta)}}\right),$$

where $C_{\text{Q},3}, C_{\text{disc}} > 0$, and η is the weak rate defined in (16), which is induced by the approximate function g_h . The parameter $0 \leq \delta \leq 1$ depends on the dimension d_2 and may depend on the smoothness of g .

Proof. We start by introducing $I_{\text{DLQ}}^{\text{ex}} = \lim_{h \rightarrow 0^+} I_{\text{DLQ}}$, the DLQMC estimator for g evaluated exactly, and further split the bias into

$$(23) \quad |\mathbb{E}[I_{\text{DLQ}}] - I| \leq \underbrace{|\mathbb{E}[I_{\text{DLQ}} - I_{\text{DLQ}}^{\text{ex}}]|}_{\text{discretization bias}} + \underbrace{|\mathbb{E}[I_{\text{DLQ}}^{\text{ex}}] - I|}_{\text{inner sampling bias}}.$$

For the discretization bias, we have

$$(24) \quad |\mathbb{E}[I_{\text{DLQ}} - I_{\text{DLQ}}^{\text{ex}}]| \leq C_{\text{disc}} h^\eta + \mathcal{O}(h^{\eta+1}),$$

where η is the weak rate defined in (16).

For the bias from the inner sampling, we first define the following:

$$(25) \quad I_Q(\{\boldsymbol{\xi}_{d_1}, \boldsymbol{\rho}_{d_1}\}) := \frac{1}{M} \sum_{m=1}^M g(\{\boldsymbol{\xi}_{d_1}, \boldsymbol{\rho}_{d_1}\}, \{\boldsymbol{\xi}_{d_2}^{(m)}, \boldsymbol{\rho}_{d_2}\}).$$

Next, we use the second-order Taylor expansion of $f(X)$ for a random variable X around $\mathbb{E}[X]$,

$$(26) \quad f(X) = f(\mathbb{E}[X]) + f'(\mathbb{E}[X])(X - \mathbb{E}[X]) + \frac{1}{2} f''(\mathbb{E}[X])(X - \mathbb{E}[X])^2 + \mathcal{O}(|X - \mathbb{E}[X]|^3),$$

to Taylor expand $f(I_Q(\{\boldsymbol{\xi}_{d_1}, \boldsymbol{\rho}_{d_1}\}))$ around $\mathbb{E}[I_Q(\{\boldsymbol{\xi}_{d_1}, \boldsymbol{\rho}_{d_1}\}) | \boldsymbol{\rho}_{d_1}] = g(\{\boldsymbol{\xi}_{d_1}, \boldsymbol{\rho}_{d_1}\})$ (with a slight abuse of notation)

$$(27) \quad \begin{aligned} f(I_Q(\{\boldsymbol{\xi}_{d_1}, \boldsymbol{\rho}_{d_1}\})) &= f(g(\{\boldsymbol{\xi}_{d_1}, \boldsymbol{\rho}_{d_1}\})) + f'(g(\{\boldsymbol{\xi}_{d_1}, \boldsymbol{\rho}_{d_1}\}))(I_Q(\{\boldsymbol{\xi}_{d_1}, \boldsymbol{\rho}_{d_1}\}) - g(\{\boldsymbol{\xi}_{d_1}, \boldsymbol{\rho}_{d_1}\})) \\ &\quad + \frac{1}{2} f''(g(\{\boldsymbol{\xi}_{d_1}, \boldsymbol{\rho}_{d_1}\})) (I_Q(\{\boldsymbol{\xi}_{d_1}, \boldsymbol{\rho}_{d_1}\}) - g(\{\boldsymbol{\xi}_{d_1}, \boldsymbol{\rho}_{d_1}\}))^2 \\ &\quad + \mathcal{O}(|I_Q(\{\boldsymbol{\xi}_{d_1}, \boldsymbol{\rho}_{d_1}\}) - g(\{\boldsymbol{\xi}_{d_1}, \boldsymbol{\rho}_{d_1}\})|^3). \end{aligned}$$

Taking the expectation conditioned on $\boldsymbol{\rho}_{d_1}$, we obtain

$$(28) \quad \mathbb{E}[f(I_Q(\{\boldsymbol{\xi}_{d_1}, \boldsymbol{\rho}_{d_1}\})) | \boldsymbol{\rho}_{d_1}] = \mathbb{E}[f(g(\{\boldsymbol{\xi}_{d_1}, \boldsymbol{\rho}_{d_1}\})) | \boldsymbol{\rho}_{d_1}] + \frac{1}{2} f''(g(\{\boldsymbol{\xi}_{d_1}, \boldsymbol{\rho}_{d_1}\})) \mathbb{V}[I_Q(\{\boldsymbol{\xi}_{d_1}, \boldsymbol{\rho}_{d_1}\}) | \boldsymbol{\rho}_{d_1}] + \mathcal{O}\left(\frac{1}{M^{2(1+\delta)}}\right),$$

where the higher-order term can be derived using the Bienaymé formula, resulting in

$$(29) \quad \begin{aligned} \mathbb{E}[I_{\text{DLQ}}] - I &= \mathbb{E}\left[\mathbb{E}[f(I_Q(\{\boldsymbol{\xi}_{d_1}, \boldsymbol{\rho}_{d_1}\})) | \boldsymbol{\rho}_{d_1}] - \mathbb{E}[f(g(\{\boldsymbol{\xi}_{d_1}, \boldsymbol{\rho}_{d_1}\})) | \boldsymbol{\rho}_{d_1}]\right] \\ &= \mathbb{E}\left[\frac{1}{2} f''(g(\{\boldsymbol{\xi}_{d_1}, \boldsymbol{\rho}_{d_1}\})) \mathbb{V}[I_Q(\{\boldsymbol{\xi}_{d_1}, \boldsymbol{\rho}_{d_1}\}) | \boldsymbol{\rho}_{d_1}]\right] + \mathcal{O}\left(\frac{1}{M^{2(1+\delta)}}\right) \\ &\leq \frac{1}{M^{(1+\delta)}} \mathbb{E}\left[\frac{1}{2} f''(g(\{\boldsymbol{\xi}_{d_1}, \boldsymbol{\rho}_{d_1}\})) \tilde{C}_{\text{Q},3}(\boldsymbol{\rho}_{d_1})\right] + \mathcal{O}\left(\frac{1}{M^{2(1+\delta)}}\right). \end{aligned}$$

□

The parameter δ can be estimated numerically along with $\tilde{C}_{\text{Q},3}(\boldsymbol{\rho}_{d_1})$ for practical applications. In addition, the constant C_{disc} in (22) might be different from that in (16).

Proposition 2 (Variance of the DLQMC estimator). *The DLQMC estimator for (12) has a variance with the following upper bound:*

$$(30) \quad \mathbb{V}[I_{\text{DLQ}}] \leq \frac{C_{\text{Q},1}}{N^{(1+\beta)}} + \frac{C_{\text{Q},2}}{NM^{(1+\delta)}} + \mathcal{O}\left(\frac{1}{N^{(1+\tilde{\beta})} M^{2(1+\delta)}}\right),$$

where $C_{\text{Q},1}, C_{\text{Q},2} > 0$ are constants and $0 \leq \beta \leq 1$ depends on the dimension d_1 and may depend on the smoothness of f , $0 \leq \delta \leq 1$ depends on the dimension d_2 and may depend on the smoothness of g , and $0 \leq \tilde{\beta} \leq 1$ depends on the dimension d_2 and may depend on the smoothness of the higher-order terms.

Proof. By the law of total variance, we have

$$(31) \quad \mathbb{V}[I_{\text{DLQ}}] = \mathbb{V}\left[\mathbb{E}\left[\frac{1}{N} \sum_{n=1}^N f(I_Q(\{\boldsymbol{\xi}_{d_1}^{(n)}, \boldsymbol{\rho}_{d_1}\})) \middle| \boldsymbol{\rho}_{d_1}\right]\right] + \mathbb{E}\left[\mathbb{V}\left[\frac{1}{N} \sum_{n=1}^N f(I_Q(\{\boldsymbol{\xi}_{d_1}^{(n)}, \boldsymbol{\rho}_{d_1}\})) \middle| \boldsymbol{\rho}_{d_1}\right]\right].$$

Using (28) for the first term yields

$$\begin{aligned}
& \mathbb{V} \left[\frac{1}{N} \sum_{n=1}^N \left(f(g(\{\boldsymbol{\xi}_{d_1}^{(n)}, \boldsymbol{\rho}_{d_1}\})) + \frac{1}{2} f''(g(\{\boldsymbol{\xi}_{d_1}^{(n)}, \boldsymbol{\rho}_{d_1}\})) \mathbb{V} \left[I_Q(\{\boldsymbol{\xi}_{d_1}^{(n)}, \boldsymbol{\rho}_{d_1}\}) \middle| \boldsymbol{\rho}_{d_1} \right] \right) \right] \\
& + \mathcal{O} \left(\frac{1}{N^{(1+\tilde{\beta})} M^{2(1+\delta)}} \right) \\
& = \mathbb{V} \left[\frac{1}{N} \sum_{n=1}^N \left(f(g(\{\boldsymbol{\xi}_{d_1}^{(n)}, \boldsymbol{\rho}_{d_1}\})) + \frac{f''(g(\{\boldsymbol{\xi}_{d_1}^{(n)}, \boldsymbol{\rho}_{d_1}\})) \tilde{D}_1(\boldsymbol{\rho}_{d_1})}{2M^{(1+\delta)}} \right) \right] + \mathcal{O} \left(\frac{1}{N^{(1+\tilde{\beta})} M^{2(1+\delta)}} \right) \\
(32) \quad & = \frac{\tilde{C}_{Q,1}}{N^{(1+\beta)}} + \mathcal{O} \left(\frac{1}{N^{(1+\tilde{\beta})} M^{2(1+\delta)}} \right).
\end{aligned}$$

Only using (27) up to the first order for the second term in (31) results in

$$\begin{aligned}
& \mathbb{E} \left[\mathbb{V} \left[\frac{1}{N} \sum_{n=1}^N \left(f(g(\{\boldsymbol{\xi}_{d_1}^{(n)}, \boldsymbol{\rho}_{d_1}\})) + f'(g(\{\boldsymbol{\xi}_{d_1}^{(n)}, \boldsymbol{\rho}_{d_1}\})) \left(I_Q(\{\boldsymbol{\xi}_{d_1}^{(n)}, \boldsymbol{\rho}_{d_1}\}) - g(\{\boldsymbol{\xi}_{d_1}^{(n)}, \boldsymbol{\rho}_{d_1}\}) \right) \right) \middle| \boldsymbol{\rho}_{d_1} \right] \right] \\
& + \mathcal{O} \left(\frac{1}{NM^{2(1+\delta)}} \right) \\
& = \mathbb{E} \left[\mathbb{V} \left[\frac{1}{N} \sum_{n=1}^N \left(f'(g(\{\boldsymbol{\xi}_{d_1}^{(n)}, \boldsymbol{\rho}_{d_1}\})) I_Q(\{\boldsymbol{\xi}_{d_1}^{(n)}, \boldsymbol{\rho}_{d_1}\}) \right) \middle| \boldsymbol{\rho}_{d_1} \right] \right] + \mathcal{O} \left(\frac{1}{NM^{2(1+\delta)}} \right) \\
(33) \quad & = \frac{\mathbb{E} \left[f'(g(\{\boldsymbol{\xi}_{d_1}, \boldsymbol{\rho}_{d_1}\}))^2 \tilde{C}_{Q,2}(\boldsymbol{\rho}_{d_1}) \right]}{NM^{(1+\delta)}} + \mathcal{O} \left(\frac{1}{NM^{2(1+\delta)}} \right).
\end{aligned}$$

□

We expect β , δ , and $\tilde{\beta}$ to be different from each other in general, as the approximated integrands might have different smoothness properties and dimensions.

With the error bounds established in Propositions (1) and (2), we can analyze the work required for the DLQMC estimator in terms of the number of samples and approximated model. We assume that the work for each model evaluation is $\mathcal{O}(h^{-\gamma})$.

Proposition 3 (Optimal work of the DLQMC estimator). *The total work of the optimized DLQMC estimator for a specified error tolerance $TOL > 0$ is given by*

$$(34) \quad W_{DLQ}^* \propto TOL^{-\left(\frac{2}{(1+\beta)} + \frac{1}{(1+\delta)} + \frac{\gamma}{\eta}\right)}$$

as $TOL \rightarrow 0$, where $0 \leq \beta \leq 1$ depends on the dimension d_1 and may depend on the smoothness of f , and $0 \leq \delta \leq 1$ depends on the dimension d_2 and may depend on the smoothness of g .

Proof. The computational work of the DLQMC estimator is

$$(35) \quad W_{DLQ} \propto NMh^{-\gamma},$$

where $h^{-\gamma}$ is proportional to the work required for evaluating g_h for discretization parameter h . The CLT allows us to approximately bound the statistical error (30) above in probability. We obtain the optimal setting by solving

$$(36) \quad (N^*, M^*, h^*, \kappa^*) = \underset{(N, M, h, \kappa)}{\arg \min} NMh^{-\gamma} \quad \text{subject to} \quad \begin{cases} \frac{C_{Q,1}}{N^{(1+\beta)}} + \frac{C_{Q,2}}{NM^{(1+\delta)}} \leq \left(\frac{\kappa TOL}{C_\alpha} \right)^2 \\ C_{\text{disc}} h^\eta + \frac{C_{Q,3}}{M^{(1+\delta)}} \leq (1 - \kappa) TOL \end{cases},$$

for $C_\alpha = \Phi^{-1}(1 - \frac{\alpha}{2})$, the inverse cdf of the standard normal at confidence level $1 - \alpha$, and $TOL > 0$ (the allotted tolerance). In addition, $\kappa \in (0, 1)$ is an error-splitting parameter.

We can solve this problem using Lagrange multipliers to derive the optimal M^* and h^* in terms of κ and N . The equation for κ^* is cubic and has a closed-form solution, but it is unwieldy to state explicitly here. The last remaining equation for N^* unfortunately has no closed-form solution for $0 < \beta < 1$, so we

must solve a simplified version and demonstrate that the resulting solution converges to the true solution as $TOL \rightarrow 0$. The optimal values are given by

$$(37) \quad M^* = \left(\frac{C_{Q,2}}{N \left(\frac{\kappa TOL}{C_\alpha} \right)^2 - \frac{C_{Q,1}}{N^\beta}} \right)^{1/(1+\delta)},$$

$$(38) \quad h^* = \left(\frac{(1-\kappa)TOL - \frac{C_{Q,3}}{C_{Q,2}} \left(N \left(\frac{\kappa TOL}{C_\alpha} \right)^2 - \frac{C_{Q,1}}{N^\beta} \right)}{C_{\text{disc}}} \right)^{1/\eta}.$$

The optimal κ^* is given by the real root of

$$(39) \quad \begin{aligned} & \left[\frac{C_{Q,3}}{C_{Q,2}} \left(\frac{NTOL}{C_\alpha} \right)^2 (\eta + \gamma(1+\delta)) \right] \kappa^{*3} + \left[NTOL \left(\eta + \frac{\gamma(1+\delta)}{2} \right) \right] \kappa^{*2} \\ & - \left[N \left(\eta TOL + \frac{C_{Q,3}}{C_{Q,2}} \frac{C_{Q,1}}{N^\beta} (\eta + \gamma(1+\delta)) \right) \right] \kappa^* - \frac{\gamma(1+\delta)C_{Q,1}C_\alpha^2}{2N^\beta TOL} = 0. \end{aligned}$$

Finally, the optimal N^* is given by the solution to

$$(40) \quad \left[\frac{C_{Q,3}}{C_{Q,2}} \left(\frac{\kappa TOL}{C_\alpha} \right)^2 \right] N^{(2+\beta)} - \left[TOL \left(1 - \kappa \left(1 + \frac{\gamma}{2\eta} \right) \right) \right] N^{(1+\beta)} - \frac{C_{Q,3}}{C_{Q,2}} C_{Q,1} N + \frac{\gamma C_\alpha^2 C_{Q,1} \beta}{2\eta \kappa TOL} = 0.$$

It immediately follows from (36) that such an N^* exists. However, it is only given in closed form for the cases $\beta \in \{0, 1\}$.

Assuming that the optimal discretization parameter h^* is independent of the sampling method (MC or RQMC), we split the bias constraint (22) as follows:

$$(41) \quad C_{\text{disc}} h^\eta \leq \frac{1}{2} (1 - \kappa) TOL,$$

$$(42) \quad \frac{C_{Q,3}}{M^{(1+\delta)}} \leq \frac{1}{2} (1 - \kappa) TOL,$$

to derive asymptotic rates in terms of the tolerance TOL . Splitting more elaborately might improve constant terms, but this is only performed for analytical purposes. Together with (38) and (37), this implies that

$$(43) \quad h^* \propto TOL^{\frac{1}{\eta}}$$

and

$$(44) \quad M^* \propto TOL^{-\frac{1}{(1+\delta)}}.$$

Next, we demonstrate that $N \propto TOL^{-\frac{2}{(1+\beta)}}$. From the variance constraint (30), we obtain

$$(45) \quad \left(\frac{\kappa TOL}{C_\alpha} \right)^2 N^{(1+\beta)} - (1 - \kappa) TOL N^\beta = C_{Q,1}.$$

The term on the right-hand side of (45) is constant in TOL . If we ignore the second term on the left-hand side, we can solve the equation (45) and obtain the approximate solution:

$$(46) \quad N \approx \left(\frac{C_\alpha^2 C_{Q,1}}{\kappa^2} \right)^{\frac{1}{(1+\beta)}} TOL^{-\frac{2}{(1+\beta)}}.$$

To determine that this approximation converges to the true solution, we check that the ignored term in (45) approaches 0 as $TOL \rightarrow 0$ as we insert (46). For this term, we have

$$(47) \quad (1 - \kappa) TOL N^\beta \approx (1 - \kappa) \left(\frac{C_\alpha^2 C_{Q,1}}{\kappa^2} \right)^{\frac{\beta}{(1+\beta)}} TOL^{1 - \frac{2\beta}{(1+\beta)}} = (1 - \kappa) \left(\frac{C_\alpha^2 C_{Q,1}}{\kappa^2} \right)^{\frac{\beta}{(1+\beta)}} TOL^{\frac{(1-\beta)}{(1+\beta)}},$$

where the exponent of TOL is between 0 and 1 because $0 < \beta < 1$. Thus, this term approaches 0 as $TOL \rightarrow 0$. In contrast, if we ignored the first term in (45), the approximate solution would be $N \approx$

$-(C_{Q,1}/(1-\kappa))^{1/\beta}TOL^{-1/\beta}$. Inserting this solution, the first term in (45) has an exponent of TOL between negative infinity and 0; thus, it approaches negative infinity as $TOL \rightarrow 0$. \square

The constants $C_{Q,1}$, $C_{Q,2}$, and $C_{Q,3}$ can be estimated using R random shifts. Rather than using the approximate solution (46), we can also solve the equation (40) numerically.

Remark 2 (Borderline settings). *In the worst case, $\beta = \delta = 0$, we obtain the optimal MC work $W_{\text{DLMC}}^* \propto TOL^{-(3+\frac{\gamma}{\eta})}$, as presented in (18). In the best case, $\beta = \delta = 1$, we obtain the optimal DLQMC work $W_{\text{DLQ}}^* \propto TOL^{-(\frac{3}{2}+\frac{\gamma}{\eta})}$, a reduction of order $3/2$ compared to the DLMC method.*

Remark 3 (Rounding optimal parameters for practical purposes). *Because of the properties of quasi-random sequences, it is beneficial to round the optimal number of samples N^* and M^* up to the nearest power of 2. The number of mesh elements is typically obtained by rounding $1/h^*$ up to the nearest integer.*

The optimal N^ provided by the numerical solution of (40) displays the predicted behavior for the fixed rates β , δ , γ , and η and constants $C_{Q,1}$, $C_{Q,2}$, $C_{Q,3}$, and C_{disc} , even for large tolerances TOL (Figure 1). Besides the DLMC and DLQMC methods (for the best case discussed in Remark 2), we also consider the case of using the RQMC method only on the inner loop ($\beta = 0, \delta = 1$). This scenario is based on the setting used in [21] and [22], except that these authors also used multilevel techniques and did not consider finite element discretization. Finally, we consider the case of using the RQMC method only on the outer loop ($\beta = 1, \delta = 0$). This setting was used in [35] and [23].*

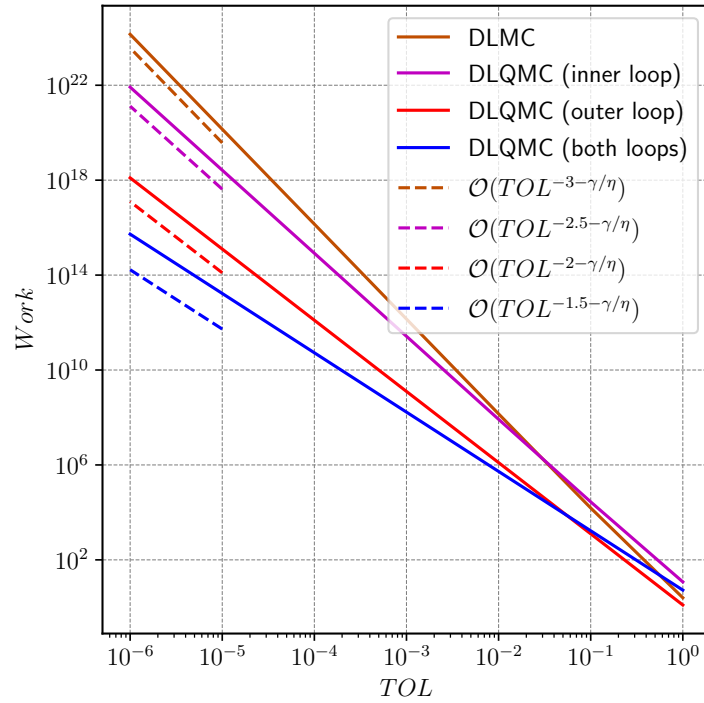


FIGURE 1. Optimal work vs. tolerance TOL for DLMC ($\beta = \delta = 0$), RQMC only on the inner loop ($\beta = 0$ and $\delta = 1$, based on the setting used in [21] and [22]), RQMC only on the outer loop ($\beta = 1$ and $\delta = 0$, this setting is used in [35] and [23]), and full DLQMC ($\beta = \delta = 1$), where $\gamma = \eta = 3$.

4. NUMERICAL RESULTS

We demonstrate the effectiveness and applicability of the derived double-loop methods for two OED problems. In particular, in Bayesian OED, the goal is to maximize the EIG of an experiment, a quantity

given by the expected Kullback–Leibler divergence of the posterior distribution of the parameters of interest $\boldsymbol{\theta}$ with respect to their prior distribution. We assume the data model

$$(48) \quad \mathbf{y}_i(\boldsymbol{\xi}) = G(\boldsymbol{\theta}_t, \boldsymbol{\xi}) + \boldsymbol{\epsilon}_i, \quad 1 \leq i \leq N_e,$$

where $\mathbf{Y} = (\mathbf{y}_1, \dots, \mathbf{y}_{N_e}) \in \mathbb{R}^{d_y \times N_e}$ is noisy data generated from the deterministic model $G : \mathbb{R}^{d_\theta} \times \mathbb{R}^{d_\xi} \rightarrow \mathbb{R}^{d_y}$ (evaluated at the true parameter vector $\boldsymbol{\theta}_t \in \mathbb{R}^{d_\theta}$) whose optimal design $\boldsymbol{\xi} \in \mathbb{R}^{d_\xi}$ we intend to find. Random observation noise is denoted $\boldsymbol{\epsilon}_i \in \mathbb{R}^{d_y}$ for N_e available independent observations under a consistent experimental setup, where d_y, d_θ, d_ξ are positive integers. The noise $\boldsymbol{\epsilon}_i$ is assumed to come from a centered normal distribution with a known covariance matrix $\boldsymbol{\Sigma}_\epsilon \in \mathbb{R}^{d_y \times d_y}$ independent of $\boldsymbol{\theta}$ and $\boldsymbol{\xi}$. Our knowledge of the parameters of interest $\boldsymbol{\theta}$ before conducting the experiment is encompassed in the prior probability density function (pdf) $\pi(\boldsymbol{\theta})$. After the experiment, our knowledge is described by the posterior pdf of $\boldsymbol{\theta}$, given by Bayes' theorem as follows:

$$(49) \quad \pi(\boldsymbol{\theta}|\mathbf{Y}, \boldsymbol{\xi}) = \frac{p(\mathbf{Y}|\boldsymbol{\theta}, \boldsymbol{\xi})\pi(\boldsymbol{\theta})}{p(\mathbf{Y}|\boldsymbol{\xi})},$$

where

$$(50) \quad p(\mathbf{Y}|\boldsymbol{\theta}, \boldsymbol{\xi}) := \det(2\pi\boldsymbol{\Sigma}_\epsilon)^{-\frac{N_e}{2}} \exp\left(-\frac{1}{2} \sum_{i=1}^{N_e} \mathbf{r}(\mathbf{y}_i, \boldsymbol{\theta}, \boldsymbol{\xi}) \cdot \boldsymbol{\Sigma}_\epsilon^{-1} \mathbf{r}(\mathbf{y}_i, \boldsymbol{\theta}, \boldsymbol{\xi})\right)$$

is the likelihood function. We omit the design parameter $\boldsymbol{\xi}$ for concision and distinguish between π for the pdfs of the parameters of interest and p for the pdfs of the data. The data residual is given by (48) as follows:

$$(51) \quad \mathbf{r}(\mathbf{y}_i, \boldsymbol{\theta}, \boldsymbol{\xi}) := \mathbf{y}_i - G(\boldsymbol{\theta}, \boldsymbol{\xi}), \quad 1 \leq i \leq N_e.$$

The amount of information regarding $\boldsymbol{\theta}$ gained from the experiment is given by

$$(52) \quad \text{EIG} := \int_{\boldsymbol{\Theta}} \int_{\mathcal{Y}} \log\left(\frac{p(\mathbf{Y}|\boldsymbol{\theta})}{\int_{\boldsymbol{\Theta}} p(\mathbf{Y}|\boldsymbol{\vartheta})\pi(\boldsymbol{\vartheta}) d\boldsymbol{\vartheta}}\right) p(\mathbf{Y}|\boldsymbol{\theta}) d\mathbf{Y} \pi(\boldsymbol{\theta}) d\boldsymbol{\theta},$$

where $\boldsymbol{\vartheta}$ is a dummy variable used for integration. Specifically, in this setting, the nonlinear outer function f in (12) is the logarithm, and the inner function g is the likelihood function.

Alternatively, we can construct an importance sampling distribution for $\boldsymbol{\vartheta}$ to reduce the variance of (quasi) MC methods [7, 8, 9, 2, 3, 10, 13, 15, 16, 17, 18]. For a thorough discussion on the Bayesian OED formulation, we refer the reader to [7, 2, 4].

Remark 4 (Closed-form expression for the numerator in the EIG). *From (51), we observe that the numerator in the logarithm in (52) only depends on $\boldsymbol{\epsilon}$ and can be computed in closed form for $\boldsymbol{\epsilon}_i \sim \mathcal{N}(\mathbf{0}, \boldsymbol{\Sigma}_\epsilon)$, $1 \leq i \leq N_e$, where $\boldsymbol{\Sigma}_\epsilon$ is a diagonal matrix in $\mathbb{R}^{q \times q}$ with entries $\sigma_{\epsilon\{j,j\}}^2$, $1 \leq j \leq q$. It is given by*

$$(53) \quad -\frac{N_e}{2} \sum_{j=1}^q \left(\log\left(2\pi\sigma_{\epsilon\{j,j\}}^2\right) + 1 \right).$$

A similar result is presented in [20], but we provide a derivation in Appendix A for completeness.

The denominator in the logarithm in (52) constitutes the inner integral of a nested integration problem to which we apply the DLQMC estimator. Alternatively, we can estimate the EIG using a single-loop MC method. The inner integral in this setting is estimated instead by a Laplace approximation. In this case, the EIG is approximated as

$$(54) \quad \text{EIG} \approx \int_{\boldsymbol{\Theta}} \int_{\mathcal{Y}} \left[\frac{1}{2} \log((2\pi)^{d_\theta} |\boldsymbol{\Sigma}|) - \frac{d_\theta}{2} - \log(\pi(\hat{\boldsymbol{\theta}})) - \frac{\text{tr}(\boldsymbol{\Sigma} \nabla_{\boldsymbol{\theta}} \nabla_{\boldsymbol{\theta}} \log(\pi(\hat{\boldsymbol{\theta}})))}{2} \right] p(\mathbf{Y}|\boldsymbol{\theta}) d\mathbf{Y} \pi(\boldsymbol{\theta}) d\boldsymbol{\theta},$$

where

$$(55) \quad \hat{\boldsymbol{\theta}} := \arg \min_{\boldsymbol{\theta}} \left[\frac{1}{2} \sum_{i=1}^{N_e} \mathbf{r}(\mathbf{y}_i, \boldsymbol{\theta}, \boldsymbol{\xi}) \cdot \boldsymbol{\Sigma}_\epsilon^{-1} \mathbf{r}(\mathbf{y}_i, \boldsymbol{\theta}, \boldsymbol{\xi}) - \log(\pi(\boldsymbol{\theta})) \right]$$

is the maximum a posteriori (MAP) estimate and

$$(56) \quad \boldsymbol{\Sigma}^{-1} := -\nabla_{\boldsymbol{\theta}} \nabla_{\boldsymbol{\theta}} G(\hat{\boldsymbol{\theta}}, \boldsymbol{\xi}) \cdot \boldsymbol{\Sigma}_\epsilon^{-1} \sum_{i=1}^{N_e} \mathbf{r}(\mathbf{y}_i, \hat{\boldsymbol{\theta}}, \boldsymbol{\xi}) + N_e \nabla_{\boldsymbol{\theta}} G(\hat{\boldsymbol{\theta}}, \boldsymbol{\xi}) \cdot \boldsymbol{\Sigma}_\epsilon^{-1} \nabla_{\boldsymbol{\theta}} G(\hat{\boldsymbol{\theta}}, \boldsymbol{\xi}) - \nabla_{\boldsymbol{\theta}} \nabla_{\boldsymbol{\theta}} \log(\pi(\hat{\boldsymbol{\theta}}))$$

is the approximate negative inverse Hessian of the log-likelihood. The MC Laplace (MCLA) and QMC Laplace (QMCLA) estimators based on (54) have a bias of $\mathcal{O}_{\mathbb{P}}\left(\frac{1}{N_e}\right)$.¹ For details, see [7, 2]. The pdf

$$(57) \quad \tilde{\pi}(\boldsymbol{\theta}|\mathbf{Y}) = \frac{1}{(2\pi)^{\frac{d_{\boldsymbol{\theta}}}{2}} |\boldsymbol{\Sigma}|^{\frac{1}{2}}} \exp\left(-\frac{(\boldsymbol{\theta} - \hat{\boldsymbol{\theta}}) \cdot \boldsymbol{\Sigma}^{-1}(\boldsymbol{\theta} - \hat{\boldsymbol{\theta}})}{2}\right)$$

can also be used as an importance sampling distribution for the inner integral in (52) (see [2]), which provides two new estimators, the DLMC estimator with importance sampling (DLMCIS) and DLQMC with importance sampling (DLQMCIS). Laplace-based importance sampling can significantly reduce the number of required inner samples for both estimators. For the construction of the QMCLA and the DLQMCIS estimator, we follow the steps in [7] and [2], respectively, replacing MC samples with RQMC samples.

Remark 5 (Number of randomizations). *To maximize the advantage of RQMC over MC, we only use one randomization in the estimator (5). Multiple randomizations $R > 1$ are only used to estimate the error (9) in a pilot run.*

4.1. Example 1: Linear example with exact sampling. For this example [29], we assume the following data model, as presented in (48):

$$(58) \quad y_i(\xi) = G(\theta_t, \xi) + \epsilon_i, \quad 1 \leq i \leq N_e,$$

where $y_i \in \mathbb{R}$ are noisy observations of the model,

$$(59) \quad G(\theta, \xi) = \theta^3 \xi^2 + \theta \exp(-|0.2 - \xi|),$$

$\xi \in [0, 1]$ is the design variable, and $\theta \sim \mathcal{U}([0, 1])$ is the parameter of interest. For the observation noise, we assume $\epsilon \sim \mathcal{N}(0, 10^{-3})$. We consider 10 experiments under the same setup; therefore, $N_e = 10$. Thus, the outer integration in (52) is $N_e \times d_y + d_{\theta} = 11$ dimensional, and the inner integration is $d_{\theta} = 1$ dimensional. The function G can be evaluated exactly; therefore, no discretization is needed.

The EIG for model (58) is displayed in Figure 2 using the DLMCIS and DLQMCIS estimators with $N = 2^{15}$ outer samples and $M = 1$ inner sample.

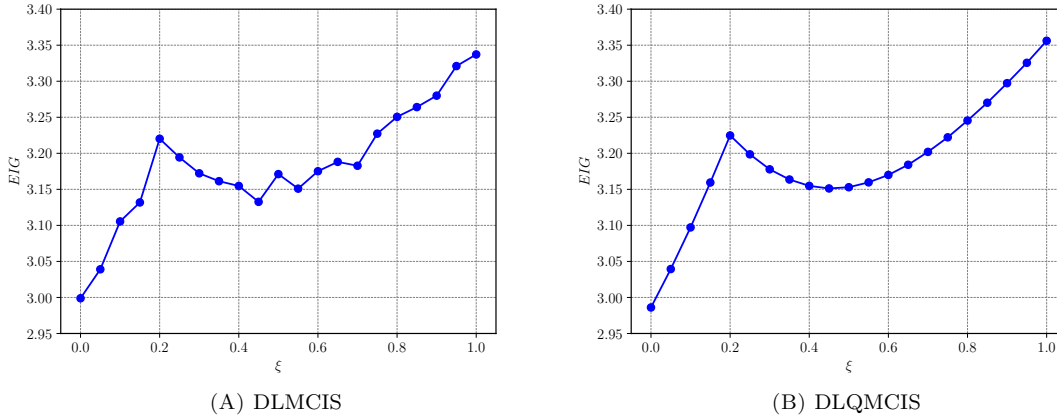


FIGURE 2. Example 1: Expected information gain (EIG) as a function of the design ξ estimated using the DLMCIS and DLQMCIS estimators with $N = 2^{15}$ outer samples and $M = 1$ inner sample.

We estimate the constants $C_{Q,1}, C_{Q,2}, C_{Q,3}, \beta$, and δ for DLQMCIS using a pilot run with $N = M = 2048$ samples and $R = 32$ randomizations. The constants $C_{QLA,1}$ and $C_{QLA,2}$, relating to the variance and bias of the QMCLA estimator, respectively, along with δ , are estimated using $N = 256$ outer samples and $R = 32$

¹We specify the notation $X_M = \mathcal{O}_{\mathbb{P}}(C_M)$ for a sequence of random variables X_M and constants C_M as follows. For any $\epsilon > 0$, there exists finite $K(\epsilon), M_0 > 0$ such that $\mathbb{P}(|X_M| > K(\epsilon)|C_M|) < \epsilon$ holds for all $M \geq M_0$.

randomizations. Figure 3 presents the rates at which the inner (N^*) and outer (M^*) numbers of samples increase as the allowed tolerance decreases. The estimation reveals that, for this example, $\beta \approx 0.84$ and $\delta \approx 0.77$. Thus, N^* increases at a rate of $2/(1 + \beta) \approx 1.09$ rather than rate 2, as is the case for DLMCIS, and M^* increases at a rate of $1/(1 + \delta) \approx 0.57$ rather than a rate of 1. Importance sampling reduces the variance of the inner estimation so that only one sample is needed for large and intermediate tolerances.

We observe that although the constants $C_{Q,2}$ and $C_{Q,3}$ are reduced significantly when using importance sampling, the rate δ deteriorates. If the importance sampling distribution (57) is optimal, the new integrand is constant. For an increasingly nonlinear G , the Laplace approximation error increases [38]; hence, the new integrand becomes less regular. This effect is more strongly observed away from the MAP point. Furthermore, the updated integrand for this example is no longer periodic, rendering RQMC less effective. For the QMCLA estimator, δ was estimated to be 1, meaning that the number of samples N increases at a rate of 1 rather than a rate of 2 as in the MCLA estimator. The bias of the QMCLA and MCLA estimators can only be reduced by increasing the number of experiments N_e ; thus, we consider it fixed. As the allowed tolerance approaches this bias, the number of required samples approaches infinity. For the pilot runs of DLMCIS and MCLA, $N = M = 2048$ samples were used. The bias from the Laplace approximation is estimated using DLQMCIS as a reference. The optimal work given by $N^* \times M^*$ is presented in Figure 4.

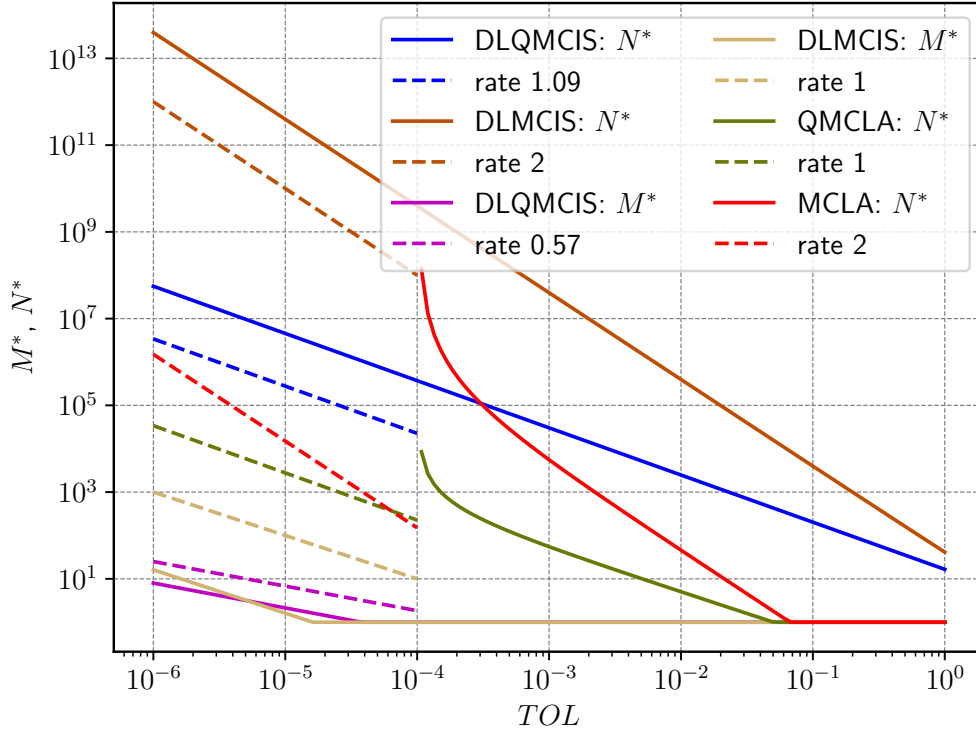


FIGURE 3. Example 1: Optimal number of the outer (N^*) and inner (M^*) samples vs. tolerance TOL for the DLQMCIS, DLMCIS, QMCLA, and MCLA estimators. Only one inner sample is needed, except for minimal tolerances due to the importance sampling. The number of required samples approaches infinity for MCLA and QMCLA as the tolerance approaches the inherent bias from the Laplace approximation.

The optimal number of inner samples M^* is rounded up to 1. Hence, the projected rate is only attained for small tolerances.

To demonstrate that the number of required samples indicated by the pilot run for the DLQMCIS estimator is sufficient for the error to be within the allowed tolerance with the specified confidence $\alpha = 0.05$,

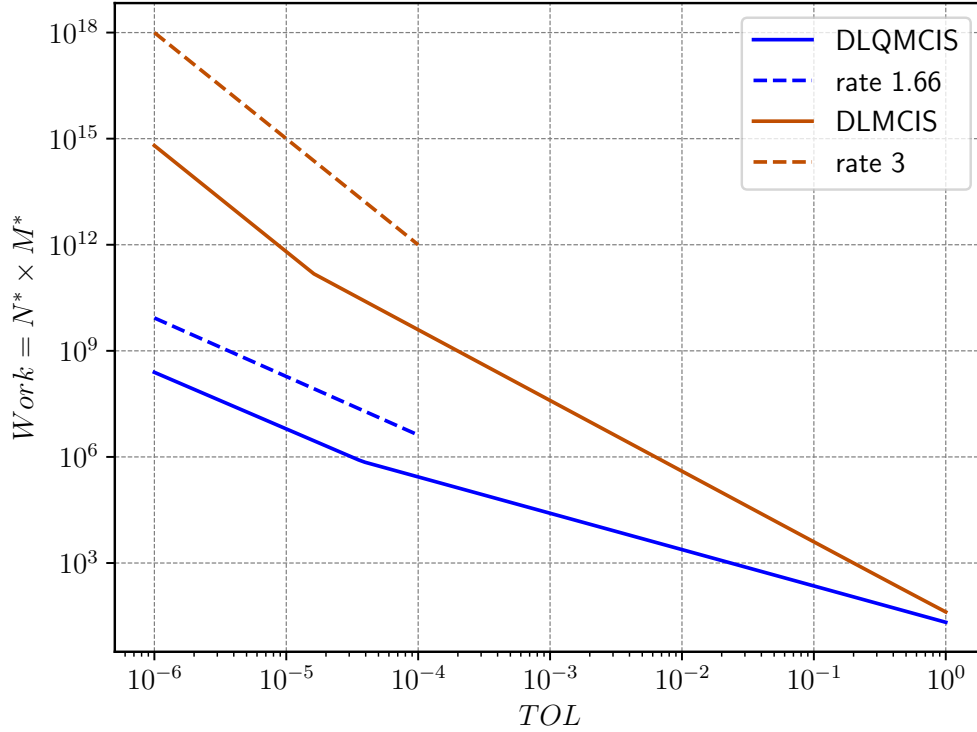


FIGURE 4. Example 1: Optimal work ($N^* \times M^*$) vs. tolerance TOL for the DLQMCIS and DLMCIS estimators. Only one inner sample is needed, except for minimal tolerances due to the importance sampling. Hence, the projected rate is only attained for small tolerances.

we ran the estimation 100 times for various tolerances $TOL = \{0.01, 0.1, 1\}$ with only one randomization $R = 1$. The results are presented in Figure 5. The error was outside the allowed tolerance only once for $TOL = 0.01$ and was always within the allowed tolerance for $TOL = 0.1$ and $TOL = 1$. The likely reason for this overconfidence is the rounding up to a power of 2 of the outer and inner samples. The mean for all runs for the least tolerance was used as a reference solution.

4.2. Example 2: Thermoelasticity example with inexact sampling. In this example, we assume that \mathbf{G} is the solution operator of a PDE; therefore, we work with an appropriate finite element approximation \mathbf{G}_h with mesh size parameter h . The domain is given by $\mathcal{D} = [0, 1]^2 \setminus \mathcal{B}(r)$, where \mathcal{B} is a ball centered at $\mathbf{0}$ with radius of 0.1 and the problem is time-dependent, with observations occurring in $t \in [0, T]$. We solve the following problem for the unknown absolute temperature ϑ (not to be confused with the dummy variable presented in (50)) and unknown displacement \mathbf{u} for fully coupled thermomechanical fields. For more information on this problem and a staggered algorithm, see [42].

A weak form of the heat equation is given by

$$(60) \quad \int_{\mathcal{D}} \rho \vartheta_0 \dot{s} \hat{\vartheta} \, d\mathcal{D} - \int_{\mathcal{D}} \mathbf{q} \cdot \nabla \hat{\vartheta} \, d\mathcal{D} = - \int_{\partial \mathcal{D}} \mathbf{q} \cdot \mathbf{n} \hat{\vartheta} \, dS \quad \forall \hat{\vartheta} \in V_{\vartheta},$$

where

$$(61) \quad \rho \vartheta_0 \dot{s} = \rho \theta_2 \dot{\vartheta} + \theta_1 (3\lambda + 2\mu) \vartheta_0 \operatorname{tr}(\dot{\epsilon}),$$

and

$$(62) \quad \mathbf{q} = -\theta_3 \nabla \vartheta.$$

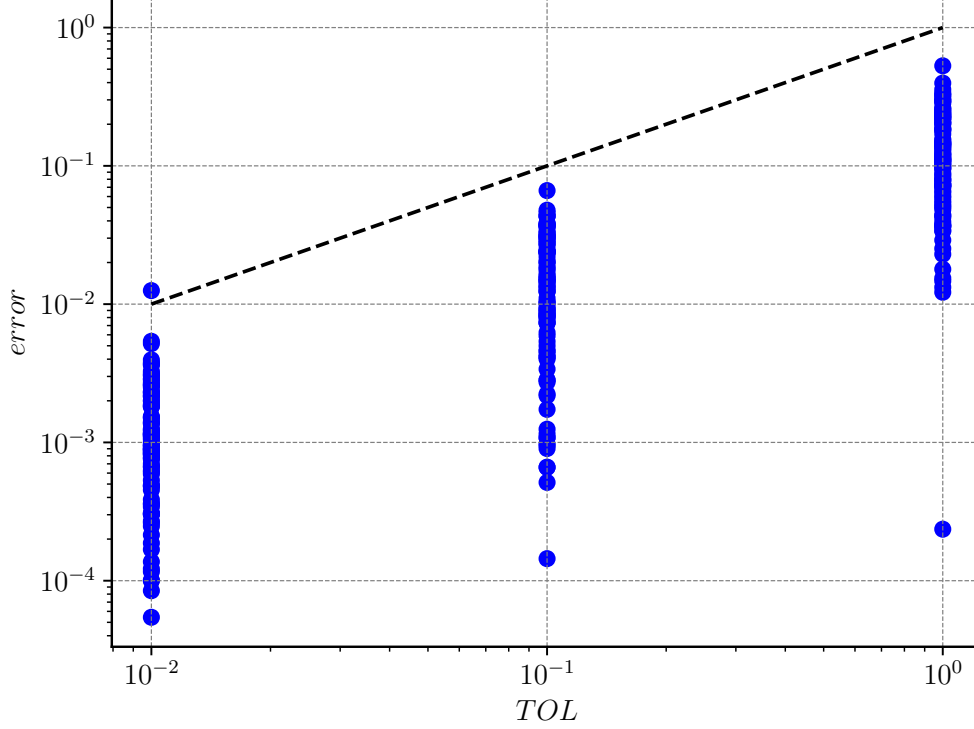


FIGURE 5. Example 1: Error vs. tolerance consistency plot. The DLQMCIS estimator stays within the allowed tolerance TOL with a predefined confidence parameter $C_\alpha = 1.96$ ($\alpha = 0.05$).

We consider $\boldsymbol{\theta} = (\theta_1, \theta_2, \theta_3) \in \mathbb{R}^3$; θ_1 , the thermal expansion coefficient; θ_2 , the specific heat per unit volume at constant strain; and θ_3 , the thermal conductivity, to be the parameters of interest. Furthermore, we consider the material density $\rho = 2700\text{kg/m}^3$, entropy per unit of mass in the current s , Lamé constants $\lambda = 7000/1.56$ and $\mu = 35000/1.3$, and initial temperature $\vartheta_0 = 293\text{K}$ to be fixed parameters. Last, we consider the strain tensor $\boldsymbol{\varepsilon} = \nabla^s \mathbf{u}$, the symmetric part of the gradient of \mathbf{u} ,

$$(63) \quad \nabla^s \mathbf{u} = \frac{1}{2}(\nabla \mathbf{u} + (\nabla \mathbf{u})^\top),$$

the unit outward normal \mathbf{n} , and the function space for the temperature field V_ϑ . For the time derivatives, we use the implicit Euler scheme. A weak form of the momentum equation is given by

$$(64) \quad \int_{\mathcal{D}} (\lambda \text{tr}(\boldsymbol{\varepsilon}) \mathbf{1} + 2\mu \boldsymbol{\varepsilon} - \theta_1(3\lambda + 2\mu)(\vartheta - \vartheta_0) \mathbf{1}) : \nabla_s \hat{\mathbf{u}} \, d\mathcal{D} = W_{\text{ext}}(\hat{\mathbf{u}}) \quad \forall \hat{\mathbf{u}} \in V_U,$$

where V_U is the function space for the displacement, $\mathbf{1}$ is the identity tensor, and W_{ext} is the linear functional corresponding to the work of body external forces and traction on the boundary. We also replace the unknown absolute temperature ϑ with the temperature variation $\Delta = \vartheta - \vartheta_0$. For this experiment, we consider a temperature increase of $\Delta = 10^\circ\text{C}$, applied at the circular exclusion. Stress and flux-free conditions are applied at the remaining boundaries, and symmetry conditions are applied on the corresponding symmetry planes. For details on the FEM, see Appendix B.

For the discretization parameter h , we chose $\lceil 1/h \rceil$, where $\lceil \cdot \rceil$ is the ceiling operator, as the mesh-resolution parameter, and the number of time steps is assumed to depend quadratically on h , (i.e., $\lceil 1/h^2 \rceil$). This is because the solution to the heat equation (60) depends linearly on time and quadratically on space. Choosing different discretization parameters h_t and h_s for time and space would enable the use of multi-index MC

techniques [43]. The actual observation times are chosen on a log scale, as the problem can be stiff initially. In addition, as the problem approaches a steady state, the observations become increasingly similar, leading to numerical issues unless the observation times are sufficiently spread apart.

For the parameters of interest θ , we assume the following prior distributions:

$$(65) \quad \theta_1 \sim \mathcal{U}(1.81, 2.81) \times 10^{-5}, \quad \theta_2 \sim \mathcal{U}(8.6, 9.6) \times 10^{-4}, \quad \theta_3 \sim \mathcal{U}(1.87, 2.87) \times 10^{-4}.$$

For the observation noise, we assume $\epsilon_i \sim \mathcal{N}(\mathbf{0}, \Sigma_\epsilon)$, $1 \leq i \leq N_e$. Moreover, Σ_ϵ is a diagonal matrix in $\mathbb{R}^{d_y \times d_y}$, where the first $d_y/2$ diagonal entries corresponding to the displacement measurements are $\sigma_{\epsilon,1}^2 = 10^{-12}$, and the second $d_y/2$ diagonal entries corresponding to the temperature measurements are $\sigma_{\epsilon,2}^2 = 10^{-8}$. The data model, as presented in (48), is given by

$$(66) \quad \mathbf{y}_i(\boldsymbol{\xi}) = \mathbf{G}_h(\boldsymbol{\theta}_t, \boldsymbol{\xi}) + \epsilon_i, \quad 1 \leq i \leq N_e,$$

where $\mathbf{y}_i \in \mathbb{R}^{d_y}$ are the noisy measurements of the displacement and temperature, and $\mathbf{G}_h(\boldsymbol{\theta}, \boldsymbol{\xi})$ is the solution operator of the discretized weak forms (60) and (64). We consider two measurements of the displacement and two measurements of the temperature at three observation times each, yielding $d_y = 12$ total observations. For $N_e = 1$ experiment, the outer integration in (52) is $N_e \times d_y + d_\theta = 15$ dimensional, and the inner integration is $d_\theta = 3$ dimensional. The domain \mathcal{D} is presented in Figure 6. There is a circular exclusion in the lower left corner. For the design parameter $\boldsymbol{\xi} = (\xi_1, \xi_2)$, we consider ξ_1 to be the position of the sensors and ξ_2 to be the maximum observation time. The sensors for the displacement are at $(0.0 + \xi_1, 1)$ and $(0.6 + \xi_1, 1)$. The sensors for the temperature are at $(0.2 + \xi_1, 1)$ and $(0.4 + \xi_1, 1)$, where $\xi_1 \in \{0.0, 0.2, 0.4\}$. Figure 7 depicts the temperature increase at observation times $t = \{10^3, 10^4\}$ for $\xi_1 = 0.2$.

Figure 8 presents the number of required optimal samples for the DLQMCIS, DLMCIS, QMCLA, and MCLA estimators obtained through pilot runs using $N = M = 64$ samples and $R = 32$ randomizations for the DLQMCIS estimator. To estimate the constants for the QMCLA estimator, $N = 256$ samples and $R = 32$ randomizations were used. For the pilot run of DLMCIS, $N = M = 128$ samples were used. Finally, the pilot for MCLA was run with $N = 1024$ samples. The resulting rates for DLQMCIS were $\beta = 0.71$ and $\delta = 0.44$. Thus, N^* increases at a rate of $2/(1 + \beta) \approx 1.17$ rather than rate 2, and M^* increases at a rate of $1/(1 + \delta) \approx 0.7$ rather than a rate of 1. Although these rates are worse than those for the previous example, they still reveal that we can exploit the regularity in the physical model and benefit from using RQMC instead of MC. For QMCLA, the estimated rate was $\delta = 1$. Thus, the number of samples N increases at a rate of 1. The bias from the Laplace approximation is again estimated using DLQMCIS as a reference. As the allowed tolerance TOL approaches the bias from the Laplace approximation, the optimal splitting parameter κ^* approaches 0 for the QMCLA and MCLA estimators. It is almost constant for the DLQMCIS and DLMCIS estimators, where the bias from the inner integration can be reduced by increasing the number of inner samples (Figure 9). The optimal work given by $N^* \times M^* \times h^{-\gamma}$ is depicted in Figure 10. The optimal number of inner samples M^* is rounded up to 1. Hence, the projected rate is only attained for small tolerances.

The EIG for model (66) is illustrated in Figure 11, where we evaluate the experiment for various sensor placements ξ_1 at observation times $t = \{10 \times \xi_2, 100 \times \xi_2, 1000 \times \xi_2\}$, $\xi_1 \in \{0.0, 0.2, 0.4\}$, and $0.5 \leq \xi_2 \leq 80$. It takes some time until the sensors start gaining sufficient information. Eventually, the process converges to a steady state, at which point the EIG decreases again. However, even for fairly large ξ_2 , the EIG is still high, which could indicate that various steady states are attained for different input parameters $\boldsymbol{\theta}$ and that the decrease in EIG only stems from the observations being almost constant in time. The highest EIG was attained for $\xi_1 = 0$, where the sensors are closest to the source in the lower left corner. For this setting, the optimal observation time was $\xi_2 = 20$. At the optimal observation time, the sensor placement has little effect on the EIG, but the sensor placement is relevant for less-than-optimal observation times. The DLQMCIS estimator for the allowed error tolerance $TOL = 0.2$ was used with only one randomization $R = 1$ and N^* , M^* , and h^* from the pilot for the EIG approximation. This tolerance necessitates a discretization parameter $h \approx 0.13$. Figure 12 illustrates the EIG for model (66) as a three-dimensional plot.

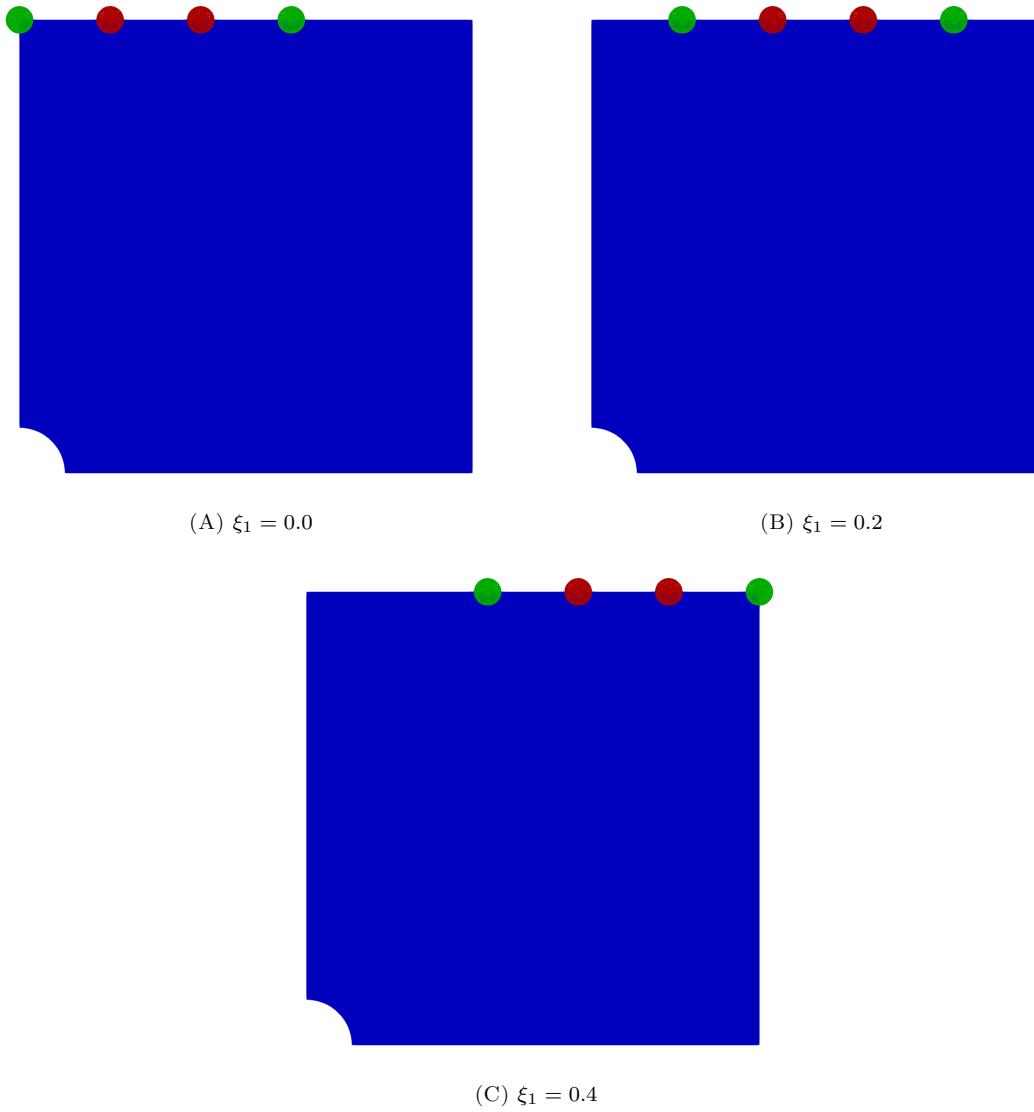


FIGURE 6. Example 2: Rectangular domain with circular exclusion and sensor locations (green marks displacement and red marks temperature).

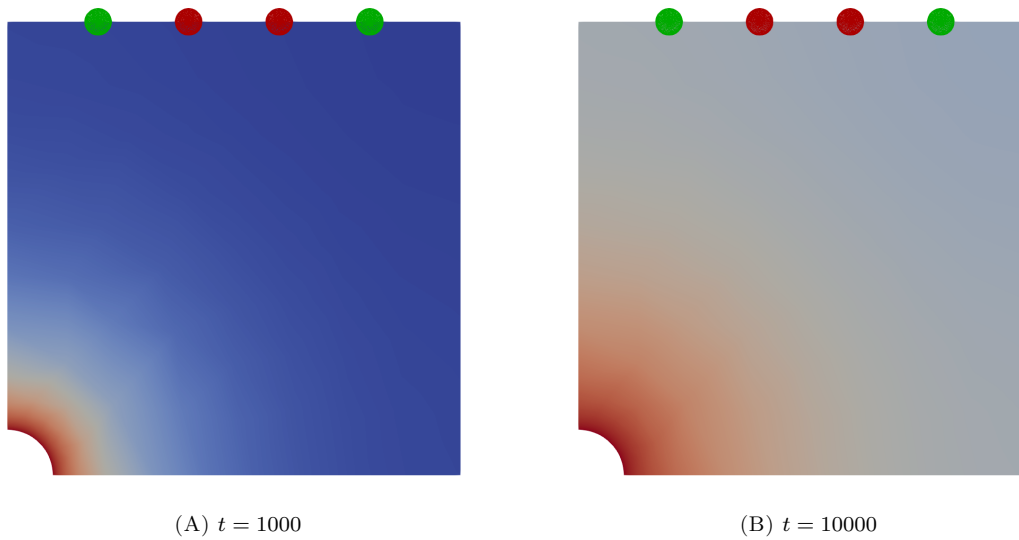


FIGURE 7. Example 2: Temperature increase at observation times of the experiment for the rectangular domain with circular exclusion. Point-sensor locations are displayed as circles at the top of the domain.

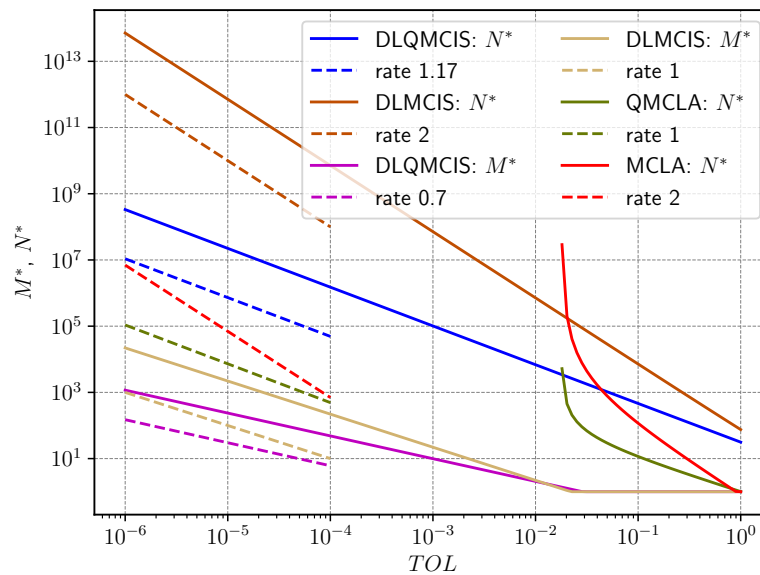


FIGURE 8. Example 2: Optimal number of the outer (N^*) and inner (M^*) samples vs. tolerance TOL for the DLQMCIS, DLMCIS, QMCLA, and MCLA estimators. The number of samples needed to reduce the variance approaches infinity for MCLA and QMCLA as the tolerance approaches the inherent bias from the Laplace approximation.

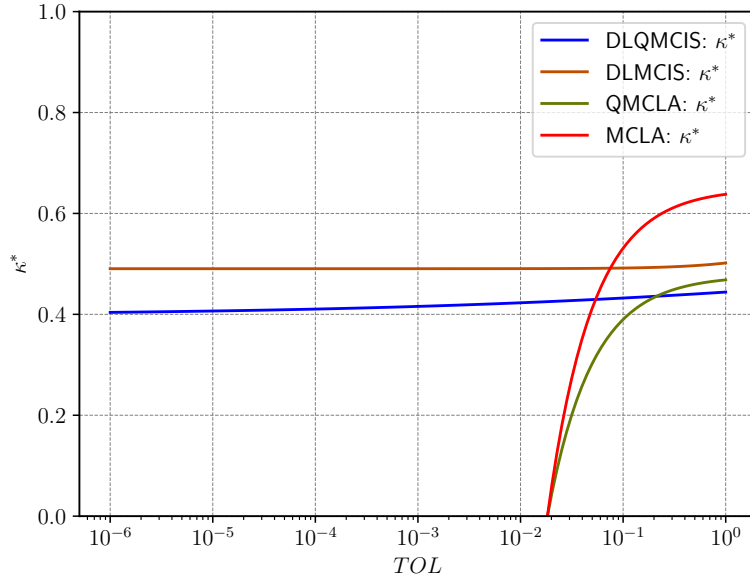


FIGURE 9. Example 2: Optimal splitting parameter (κ^*) vs. tolerance TOL for the DLQMCIS, DLMCIS, QMCLA, and MCLA estimators. The optimal κ^* approaches zero for the MCLA and QMCLA estimators as the tolerance approaches the inherent bias from the Laplace approximation.

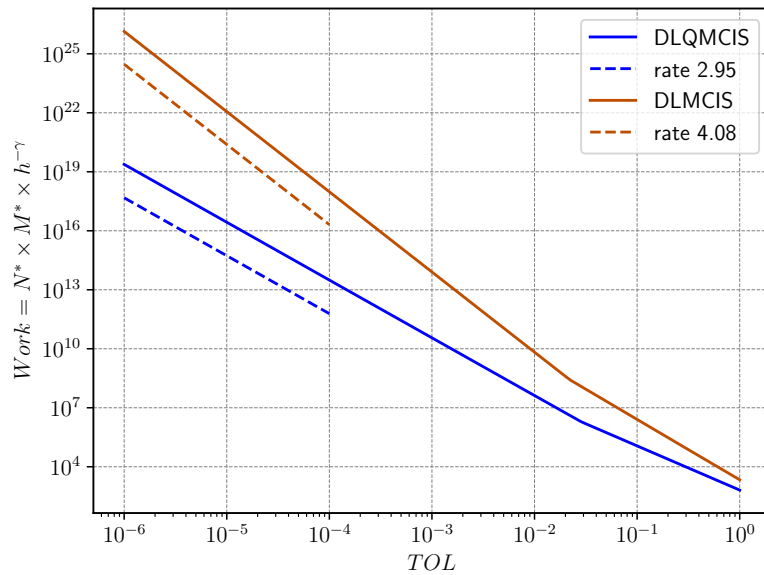


FIGURE 10. Example 2: Optimal work ($N^* \times M^* \times h^{-\gamma}$) vs. tolerance TOL for the DLQMCIS and DLMCIS estimators. Only one inner sample is needed, except for minimal tolerances due to the importance sampling. Hence, the projected rate is only attained for small tolerances.

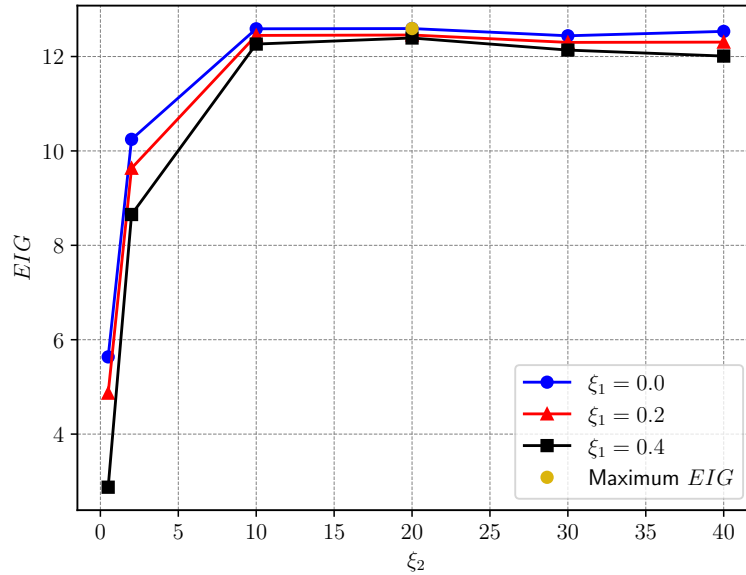


FIGURE 11. Example 2: Expected information gain (EIG) as a function of the design ξ , estimated with the DLQMCIS estimator with an allowed tolerance of $TOL = 0.2$. The maximum EIG is reached for $\xi_1 = 0$ and $\xi_2 = 20$ (highlighted in gold).

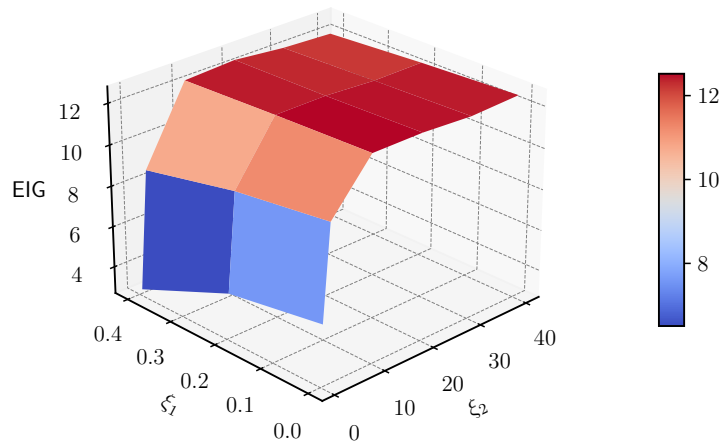


FIGURE 12. Example 2: Expected information gain (EIG) as a function of the design ξ , estimated with the DLQMCIS estimator with an allowed tolerance of $TOL = 0.2$. The maximum EIG is reached for $\xi_1 = 0$, $\xi_2 = 20$.

5. CONCLUSION

We propose estimating nested integrals using randomized quasi-Monte Carlo (RQMC) approximations for the outer and inner integrals, furnishing the double-loop quasi-Monte Carlo estimator (DLQMC). For this method, we derive asymptotic error bounds and obtain the optimal number of samples required for each approximation as the main contribution of the work. Application to Bayesian optimal experimental design indicates that this method is superior to using the RQMC method for only one or neither integral approximation. Replacing the inner integral with the Laplace approximation yields an even more efficient estimator but is only feasible for large error tolerances. For small tolerances, a Laplace-based importance sampling for the inner integral further improves the advantages of the proposed DLQMC estimator.

6. ACKNOWLEDGMENTS

This publication is based upon work supported by the King Abdullah University of Science and Technology (KAUST) Office of Sponsored Research (OSR) under Award No. OSR-2019-CRG8-4033, the Alexander von Humboldt Foundation, the Deutsche Forschungsgemeinschaft (DFG, German Research Foundation) – 333849990/GRK2379 (IRTG Modern Inverse Problems), and was partially supported by the Flexible Interdisciplinary Research Collaboration Fund at the University of Nottingham Project ID 7466664.

APPENDIX A. PROOF OF REMARK 4

Proof. We first assume that $N_e = q = 1$. From (50), the numerator in the logarithm in (52) is given by the following:

$$(67) \quad \begin{aligned} & \int_{\mathbb{R}} \log \left(\frac{1}{\sqrt{2\pi\sigma_\epsilon^2}} \exp \left(-\frac{\epsilon^2}{2\sigma_\epsilon^2} \right) \right) \frac{1}{\sqrt{2\pi\sigma_\epsilon^2}} \exp \left(-\frac{\epsilon^2}{2\sigma_\epsilon^2} \right) d\epsilon \\ &= -\frac{1}{2} \log(2\pi\sigma_\epsilon^2) - \frac{1}{\sqrt{2\pi\sigma_\epsilon^2}} \frac{1}{2\sigma_\epsilon^2} \int_{\mathbb{R}} \epsilon^2 \exp \left(-\frac{\epsilon^2}{2\sigma_\epsilon^2} \right) d\epsilon. \end{aligned}$$

We can write $s := 1/(2\sigma_\epsilon^2)$ and solve the integral in (67) by taking the derivative with respect to s :

$$(68) \quad \begin{aligned} \int_{\mathbb{R}} \epsilon^2 e^{-s\epsilon^2} d\epsilon &= -\int_{\mathbb{R}} \frac{\partial}{\partial s} e^{-s\epsilon^2} d\epsilon = -\frac{\partial}{\partial s} \int_{\mathbb{R}} e^{-s\epsilon^2} d\epsilon = -\sqrt{\pi} \frac{\partial}{\partial s} s^{-\frac{1}{2}} \\ &= \sqrt{\frac{\pi}{s}} \frac{1}{2s} = \sqrt{2\pi\sigma_\epsilon^2} \sigma_\epsilon^2. \end{aligned}$$

Inserting this back into (67) changes the numerator in (52) to $-(\log(2\pi\sigma_\epsilon^2) + 1)/2$. The case for $\epsilon_i \in \mathbb{R}^q$, $1 \leq i \leq N_e$, follows trivially under the hypothesis. \square

APPENDIX B. DERIVATION OF THE FINITE ELEMENT FORMULATION

We let $(\Omega, \mathcal{F}, \mathbb{P})$ be a complete probability space with outcomes Ω , σ -field \mathcal{F} , and probability measure \mathbb{P} . We define $\mathcal{H} := H^1(\mathcal{D} \times \mathcal{D})$ as the space of the solution for the coupled thermomechanical fields $(\vartheta(\omega), \mathbf{u}(\omega))$ for $\omega \in \Omega$. In addition, $H^1(\mathcal{D} \times \mathcal{D})$ is the standard Sobolev space $W^{1,2}(\mathcal{D} \times \mathcal{D})$ with corresponding Sobolev norm. Furthermore, we define the Bochner space as follows:

$$(69) \quad V_\vartheta \times V_U \equiv L_{\mathbb{P}}^2(\Omega; \mathcal{H}) := \left\{ (\vartheta, \mathbf{u}) : \Omega \rightarrow \mathcal{H} \quad \text{s.t.} \quad \left(\int_{\Omega} \|\vartheta(\omega), \mathbf{u}(\omega)\|_{\mathcal{H}}^2 d\mathbb{P}(\omega) \right)^{1/2} < \infty \right\}.$$

We aim to determine $(\vartheta, \mathbf{u}) \in L_{\mathbb{P}}^2(\Omega; \mathcal{H})$ such that the weak formulations (60) and (64) are fulfilled for all $(\hat{\vartheta}, \hat{\mathbf{u}}) \in L_{\mathbb{P}}^2(\Omega; \mathcal{H})$.

REFERENCES

- [1] Ryan KJ. Estimating expected information gains for experimental designs with application to the random fatigue-limit model. *Journal of Computational and Graphical Statistics*, 12:585–603, 2003.
- [2] Beck J, Dia BM, Espath LF, Long Q, and Tempone R. Fast Bayesian experimental design: Laplace-based importance sampling for the expected information gain. *Computer Methods in Applied Mechanics and Engineering*, 334:523–553, 2018.
- [3] Beck J, Dia BM, Espath LF, and Tempone R. Multilevel double loop Monte Carlo and stochastic collocation methods with importance sampling for Bayesian optimal experimental design. *International Journal for Numerical Methods in Engineering*, 121:3482–3503, 2020.

- [4] Carlon AG, Dia BM, Espath LF, Lopez RH, and Tempone R. Nesterov-aided stochastic gradient methods using Laplace approximation for Bayesian design optimization. *Computer Methods in Applied Mechanics and Engineering*, 363:112909, 2020.
- [5] Shannon CE. A mathematical theory of communication. *Bell System Technical Journal*, 27:379–423, 1948.
- [6] Kullback S. *Information theory and statistics*. Wiley, 1959.
- [7] Long Q, Scavino M, Tempone R, and Wang S. Fast estimation of expected information gains for Bayesian experimental designs based on Laplace approximations. *Computer Methods in Applied Mechanics and Engineering*, 259:24–39, 2013.
- [8] Long Q. Multimodal information gain in Bayesian design of experiments. *arXiv preprint arXiv:2108.07224*, 2021.
- [9] Schillings C, Sprungk B, and Wacker P. On the convergence of the Laplace approximation and noise-level-robustness of Laplace-based Monte Carlo methods for Bayesian inverse problems. *Numerische Mathematik*, 145:915–971, 2020.
- [10] Wacker P. Laplace’s method in Bayesian inverse problems. *arXiv preprint arXiv:1701.07989*, 2017.
- [11] Chaloner K and Verdinelli I. Bayesian experimental design: a review. *Statistical Sciences*, 10:273–304, 1995.
- [12] Kullback S and Leibler RA. On information and sufficiency. *Annals of Mathematical Statistics*, 22:79–86, 1951.
- [13] Stigler SM. Laplace’s 1774 memoir on inverse probability. *Statistical Science*, 1:359–378, 1986.
- [14] Lindley DV. On a measure of information provided by an experiment. *Annals of Mathematical Statistics*, 27:986–1005, 1956.
- [15] Tierney L and Kadane JB. Accurate approximations for posterior moments and marginal densities. *Journal of the American Statistical Association*, 81:82–86, 1986.
- [16] Tierney L, Kass RE, and Kadane JB. Fully exponential Laplace approximations to expectations and variances of nonpositive functions. *Journal of the American Statistical Association*, 84:710–716, 1989.
- [17] Kass RE, Tierney L, and Kadane JB. The validity of posterior expansions based on Laplace’s method. in: *Geisser S, Hodges JS, Press SJ, and Zellner A (Eds.), Essays in Honor of George Barnard*, 473–488, 1990.
- [18] Long Q, Scavino M, Tempone R, and Wang S. A Laplace method for under-determined Bayesian optimal experimental designs. *Computer Methods in Applied Mechanics and Engineering*, 285:849–876, 2015.
- [19] Giles MB. Multilevel Monte Carlo path simulation. *Operations Research*, 56(3):607–617, 2008.
- [20] Tsilifis P, Ghanem RG, and Hajali P. Efficient Bayesian experimentation using an expected information gain lower bound. *SIAM/ASA Journal on Uncertainty Quantification*, 5:30–62, 2017.
- [21] Goda T, Daisuke M, Kei T, and Kozo S. Decision-theoretic sensitivity analysis for reservoir development under uncertainty using multilevel quasi-Monte Carlo methods. *Computational Geosciences*, 22:1009–1020, 2018.
- [22] Xu Z, He Z, and Wang X. Efficient risk estimation via nested multilevel quasi-Monte Carlo simulation. *arXiv preprint arXiv:2011.11898*, 2020.
- [23] Fang W, Wang Z, Giles MB, Jackson CH, Welton NJ, Andrieu C, and Thom H. Multilevel and quasi Monte Carlo methods for the calculation of the expected value of partial perfect information. *Medical Decision Making*, 42(2):168–181, 2022.
- [24] Caflisch RE. Monte Carlo and quasi-Monte Carlo methods. *Acta Numerica*, 1–49, 1998.
- [25] Hickernell FJ. Lattice rules: How well do they measure up? In: *Hellekalek P and Larcher G (Eds.). Random and Quasi-Random Point Sets. Lecture Notes in Statistics 138*, New York, Springer, 109–166, 1998.
- [26] Niederreiter H. Random number generation and quasi-Monte Carlo methods. *SIAM*, Philadelphia, 1992.
- [27] Owen AB. Quasi-Monte Carlo sampling. In: *Monte Carlo Ray Tracing: SIGGRAPH*, 69–88, 2003.
- [28] Tuffin B. Randomization of quasi-Monte Carlo methods for error estimation: survey and normal approximation. In: *Monte Carlo Methods and Applications*, De Gruyter, 10(3-4):617–628, 2004.
- [29] Huan X and Marzouk YM. Simulation-based optimal Bayesian experimental design for nonlinear systems. *Journal of Computational Physics*, 232:288–317, 2013.
- [30] Durrett R. Probability: Theory and examples. *Cambridge University Press*, 2019.
- [31] Dick J and Pillichshammer F. Digital nets and sequences: discrepancy theory and quasi-Monte Carlo integration. *Cambridge University Press*, 2010
- [32] Loh WL. On the asymptotic distribution of scrambled net quadrature. *The Annals of Statistics*, 31(4):1282–1324, 2003.
- [33] Dick J, Kuo FY, and Sloan IH. High-dimensional integration: the quasi-Monte Carlo way. *Acta Numerica*, 133–288, 2013.
- [34] Sobol’ IM. Distribution of points in a cube and approximate evaluation of integrals. *Ž. Vyčisl. Mat. i Mat. Fiz. (in Russian)*, 7:784–802, 1967.
- [35] Drovandi CC and Tran M-N. Improving the efficiency of fully Bayesian optimal design of experiments using randomised Quasi-Monte Carlo. *Bayesian Analysis*, 13(1):139–162, 2018.
- [36] L’Ecuyer P, Munger D, and Tuffin B. On the distribution of integration error by randomly-shifted lattice rules. *Electronic Journal of Statistics*, 4:950–993, 2010.
- [37] Gobet E, Lerasle M, and Métivier D. Mean estimation for randomized Quasi Monte Carlo method. *Hal preprint hal-03631879v2*, 2022.
- [38] Helin T and Kretschmann R. Non-asymptotic error estimates for the Laplace approximation in Bayesian inverse problems. *Numerische Mathematik*, 150:521–549, 2022.
- [39] L’Ecuyer P. Randomized Quasi-Monte Carlo: An introduction for practitioners. In: *Owen A and Glynn P (Eds.). Monte Carlo and Quasi-Monte Carlo Methods. MCQMC 2016. Springer Proceedings in Mathematics & Statistics*, Cham, Springer 241:29–52, 2018.
- [40] Hlawka E. Funktionen von beschränkter Variation in der Theorie der Gleichverteilung. *Annali di Matematica Pura ed Applicata*, 54:325–333, 1961.
- [41] Owen AB. Local antithetic sampling with scrambled nets. *The Annals of Statistics*, 36(5):2319–2343, 2008.

- [42] Farhat C, Park KC, and Dubois-Pelerin Y. An unconditionally stable staggered algorithm for transient finite element analysis of coupled thermoelastic problems. *Computer Methods in Applied Mechanics and Engineering*, 85(3):349–365, 1991.
- [43] Haji-Ali A-L, Nobile F, Tamellini, L, and Tempone R. Multi-index stochastic collocation convergence rates for random PDEs with parametric regularity. *Foundations of Computational Mathematics*, 16:1555–1605, 2016.